Development and analysis of beta glucan particles for high throughput peptide and protein loading

University of Massachusetts Medical School Project Center

5/1/2014

A Major Qualifying Project:
Submitted to the faculty
of the Worcester Polytechnic Institute
in partial fulfillment of the requirements
for the Degree of Bachelor of Science
by:

Zachary Duca:_____

and

Lindsay Jones:_____

Approved by:

Gary Ostroff Ph.D.:_____
UMass Medical School Project Advisor
Program in Molecular Medicine

Samuel Politz Ph.D.:_____
WPI Major Advisor
Department of Biology and Biotechnology

1. Molecular Medicine
2. Nanotechnology
3. High-throughput

Destin Heilman Ph.D.:_____
UMass Medical School Project Center Director
Department of Chemistry and Biochemistry

1 Abstract

A procedure for protein and peptide loading using beta glucan particles (GPs) had been developed been developed that required repetitive mixing in small volumes in tubes (Huang et. al, 2010). The goal of this project was to increase the efficiency of this protein encapsulation process by developing high throughput loading conditions in 96-well plates. Once ideal conditions for high-throughput loading methods were established, we evaluated methods to load cysteine-containing peptide binding using GPs derivatized with the heterobifunctional cross linker N-succinimidyl S-acetylthioacetate (SATA, 231.23 g.mol) and a new activated thiol crosslinking method with 2,2'-dithiolethyl bis(4-azido-2,3,5,6-tetrafluorobenzoate) (DAT, 224.25 g/mol). Further analysis of peptide loading was done using fluorescent and N-Pyr(Cys) peptide binding, and *in vitro* immunological experiments. The results of the 96-well plate loading method demonstrated that the best method for high-throughput loading was, in fact an adaptation of the original procedure for loading beta glucan particles in particles in 96-well plates. This method loaded proteins in fifty percent of the hydrodynamic volume of the particles followed by a water push of twenty-five percent of the hydrodynamic volume and trapping inside GPs as an albumin-yeast RNA nanocomplex. Analysis of both the SATA cross linker method and the new approach using DAT revealed that the SATA-derivatized particles had a higher degree of functionalization in comparison to the DAT-derivatized particles. Ellman's Assay used to measure incorporated thiol onto the branched polyethyleneimine-labeled SATA particles showed 7.10×10^4 molecules of thiol bound per GP, while DAT particles showed 7.00×10^3 molecules of thiol bound per GP. Immunological testing for GP mediated peptide delivery to dendtritic cell-OT-II T-cells is underway. Immunological testing to assess the functional activity of GP-peptide linked through linear PEI/SATA versus DAT revealed that DAT-derivatized GPs stimulated a stronger immune

response in murine OT-II cells than linear PEI/SATA-derivatized GPs. In addition, immunological testing to assess the functional activity of Ova protein-loaded GPs versus IgG- and lysozyme-loaded GPs showed that GPs loaded with Ova protein and with IgG, both in the 96-well plate and in tubes, stimulated a T-cell response.

2 Acknowledgements

We would like to thank our advisor Gary Ostroff and Zu Ting Shen for all their resources, guidance, and assistance in maintaining the overall success of this project. We would like to thank our advisor Samuel Politz for keeping this project on track through regular check-ins. We would like to thank Destin Heilman for approving and directing this project through the University of Massachusetts Medical School (UMMS). We would like to give a special thanks to the laboratory of Dr. Yan MingDi of the University of Massachusetts at Lowell for allowing us to utilize needed laboratory equipment. We would like to thank Jessica Cohen in the Czech lab at UMMS for her collaboration in peptide binding research. Lastly, we would like to thank Dr. Haibin Huang in the Levitz Lab at the UMMS for performing the *in vitro* OT-II T-cell proliferation assays.

3 Table of Contents

4 Table of Figures

5 Table of Tables

6 Introduction

6.1 Immune System

The immune system of vertebrates is designed to respond to microbes that could pose a threat to the organism. There are two branches of the immune system, innate immunity and adaptive immunity, which make up this defense. The innate immune system is designed to respond immediately to infection and is mostly made up of phagocytic cells, such as neutrophils and macrophages, which are activated by pathogens via germ-line encoded receptors. These cells recognize structures found on most microorganisms, such as PAMPs (pathogen associated molecular patterns), and are responsible for destroying infected cells and pathogens (Akira & Hemmi, 2003). The innate immune system can also produce cytokines and chemokines, which activate adaptive immunity (Clark, Kerrigan & Brown, 2011).

The adaptive immune system is largely made up of B- and T-cells. B-cells play a large role in host defense by either serving as an antigen presenting cell to activate T-cells or by producing antibodies which will neutralize foreign antigens. After antigen clearance, a small number of effector B-cells develop into memory B-cells, which allow for quick recall responses to the initially encountered antigen (LaRosa & Orange, 2008). This feature is known as immunological memory and is the hallmark of the adaptive immune system.

There are several subsets of T-cells, including helper T-cells and cytotoxic T-cells. Helper T-cells serve several roles, including the maturation of B-cells or the activation of cytotoxic T-cells. Helper T-cells are activated to produce cytokines upon recognition of foreign antigens presented by MHC class II molecules on the surface of antigen presenting cells. In contrast to helper T-cells, the main role of cytotoxic T-cells is to kill virally-infected cells or cancer cells. Cytotoxic T-cells recognize MHC class I molecules presenting foreign and self-antigens. Like B-

cells, a subset of helper and cytotoxic T-cells develop into long lasting memory T-cells that can be rapidly reactivated when challenged with the original antigen.

6.2 Vaccines

The major goal of vaccination is to help prevent subsequent infections. Vaccines were first developed by Edward Jenner who realized that milkmaids who were previously exposed to cowpox were protected against smallpox. The common practice for protecting against smallpox at the time was variolation, a practice where smallpox matter was introduced to a patient in order to prevent them from getting the disease. Unfortunately, this practice caused some patients to get the disease, which occasionally began a small epidemic. When Jenner realized cowpox made a person immune to smallpox, he introduced matter from a fresh cowpox lesion to a boy and then later introduced matter from a smallpox lesion. The boy did not get smallpox, so Jenner concluded that the protection was complete (Riedel, 2005). Vaccines are designed to generate immunological memory, so that memory B and T cells can quickly be activated when the body becomes re-infected with a pathogen containing the previously exposed to antigen. Vaccines can be developed using components from a given pathogen such as crude extracts, proteins, MAPs, and peptides (Huang et. al, 2010).

6.3 Beta-Glucan Particles

Beta-glucan particles (GPs) are 3-4μm hollow particles extracted from *Saccharomyces cerevisiae* (baker's yeast). Beta-glucan particles are prepared by treating the walls of the yeast cells so that the cell wall components and soluble proteins are removed. GPs are composed of β-1-3-D-glucan and residual chitin (Yan et al., 2005). These GPs can be loaded with payload molecules and

used to deliver these molecules into a cell (Brown and Gordon, 2001). Receptors on the surface of phagocytic cells, dectin-1 and Complement Receptor-3 (or CR3), recognize beta-glucans, allowing targeted delivery of the drug into macrophages and dendritic cells (Sanders and Hendrin, 1997). The use of GPs for the delivery of macromolecules, such as DNA, siRNAs, and protein antigens, has been successfully demonstrated both *in vitro* and *in vivo* (Soto and Ostroff, 2008; Aouadi et al., 2009).

6.4 Protein Loading Method

The standard method for loading and trapping macromolecules inside the porous β -glucan particles involves hand mixing the macromolecule in a volume of liquid completely absorbed by the hollow sponge-like glucan particles inside a microcentrifuge tube. This initial step is followed by several "water-push" steps where water is mixed with the lyophilized GP protein powder in the tube in order to push by capillary action a greater percentage of the macromolecules inside the GP, altering the concentration gradient across the porous surface. The molecules are then trapped inside the GP by an albumin-yeast RNA nanocomplex, allowing the molecules to remain inside the particle until the substance is released by proteolysis in the phagolysosome after having been taken up by a phagocytic cell (Huang et. all, 2010). A visual representation of this can be seen in Figure 1. The use of yeast RNA as a trapping polymer for macromolecules in β-glucan particles was demonstrated by Ostroff and typical encapsulation efficiencies of 95+% are attainable. This laborious hands-on tube method of GP loading, however, is not well suited for high-throughput loading to build GP peptide or protein antigen libraries (Negmetzhanov, 2012).

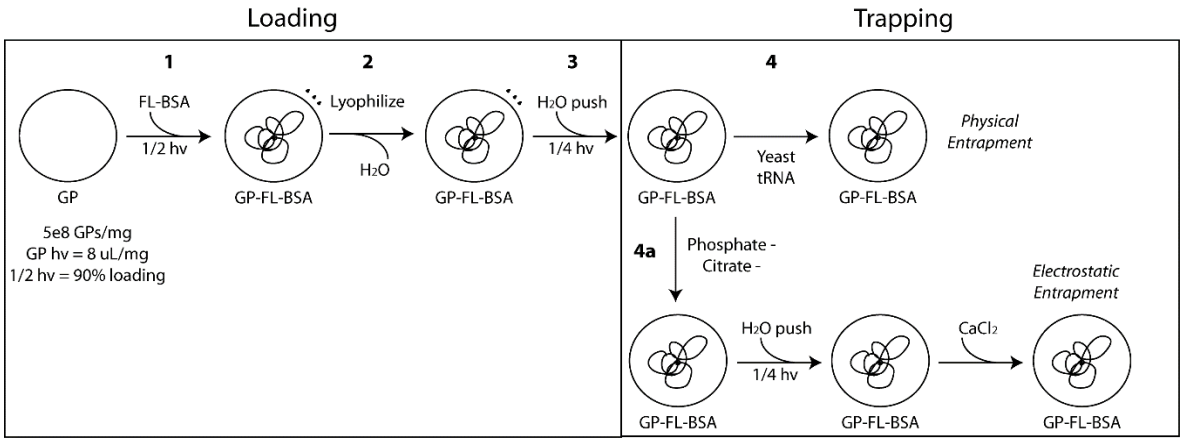

Figure 1: Standard loading of proteins into GPs

6.5 Peptide Binding Method

In addition to loading molecules inside the GPs, chemically active residues can be bound to the GP shells. This option provides an alternative method for GP payload delivery and was investigated as a way to better load peptides because the peptides do not bind well in the albumin tRNA matrix used for trapping molecules inside the GPs. To study this idea, different techniques of binding peptides to the surface were examined (Negmetzhanov, 2012).

6.6 SATA Modified GP Binding Method

β-glucan particles can be derivatized with various molecules to allow peptides and other such molecules to be bound to the surface for delivery to macrophage cells. To activate the neutral glucan polysaccaride particles, different cationic polymers, such as chitosan or PEI, can be added to the surface of GPs to establish an electrostatic or covalent payload binding mechanism. These cationic Polyethyleneimine-GPs and Chitosan-GPs can then have their surface further derivatized with N-Sucinimidyl S-Acetylthioacetate (SATA), a sulfhydryl-containing modification reagent that reacts with primary amines (-NH2). Such amines are found on the side chain of antibodies and

proteins. Treating protected sulfhydryl groups created by SATA with hydroxylamine yields free sulfhydryl groups. These sulfhydryl groups are then used for disulfide bond conjugation reactions to bind thiol-containing Cysteine-peptides. Binding peptides to the surface of the GPs is a way to deliver the peptides to macrophages, which can be used for practical applications, such as vaccines. Unfortunately, this covalent linking method also produces ionic interaction side products that must be removed by performing a salt wash. This step could potentially be eliminated by developing a method that does not form these undesirable ionic interactions (Negmetzhanov, 2012).

6.7 DAT

One possible alternative to surface derivitization with SATA was to use a diazido compound. To attempt this process, the compound 2,2'-dithiolethyl bis(4-azido-2,3,5,6-tetrafluorobenzoate) (DAT) was made. When exposed to UV radiation, the azide group of this compound breaks down, forming a nitrene that can directly attach to hydroxyls on the GP surface (Ohana et. al., 1995). However, DAT is not water soluble, so other solvents must be used. Additionally, the UV radiation necessary for breaking down this compound can be harmful for the GPs and prolonged exposure could cause them to break apart. Therefore, minimization of this exposure is essential. If these obstacles can be surmounted, then this method could be cheaper, faster, and more efficient then SATA modified GP coupling.

6.8 OT-II T-cell Proliferation

The unique structure of GPs allows recognition and uptake by phagocytic dendritic cells or macrophages (APCs; antigen presenting cells). We took advantage of transgenic T-cell mice containing CD4+ OT-II T-cells, which specifically recognize Ova protein or peptide as an MHC-

II antigen. CD4+ OT-II T cells can be used for quantifying the functional response towards Ova core-loaded and Ova surface-bound GPs when used processed and presented by phagocytic APCs. The APCs recognize, uptake, and digest GPs along with the Ova payload for presentation to CD4+ OT-II T-cells. Once introduced to the Ova antigen, the T-cells mount an immune response and proliferate, which can be measured using a [^{3}H]-thymidine T-cell proliferation assay (Huang et al., 2010). Using this assay, we tested different N-Pyr(Cys) peptide Ova-surface linked GP samples utilizing the GP core loaded Ova sample as a control.

7 Project Goals

Vaccines are some of the most important methods for preventing infectious disease. β-glucan particles (GPs) have been shown to be an effective method for delivery macromolecules. The first goal of this project was to develop a high-throughput method to load GPs with proteins in 96-well plates and to examine loading efficiency and biological activity of these particles. The second goal of this experiment was to bind peptides to the surface of GPs as an alternative to GP-core loading. One such method is a GP-$(NH_2)_n$ + SATA reaction, which, unfortunately, results in ionic interactions between N-Pyr(Cys) peptides and charged amine residues, preventing desired covalent linkages between SATA and the peptides. Optimization of the GP-$(NH_2)_n$ + SATA reaction to saturate all primary amines and greatly increase overall peptide binding efficiency would be the desired outcome. In coordination with the second goal, a third objective was to examine an alternative conjugation approach using a newly synthesized compound 2,2'-dithiolethyl bis(4-azido-2,3,5,6-tetrafluorobenzoate) for direct peptide linkage onto the surface of GPs. GP-core loaded Ova protein and GP-surface linked Ova peptide were tested using an OT-II T-cell assay for biological activity. This assessment allows comparison of these different protein/peptide vaccine delivery strategies, culminating all experiments.

8 Materials

8.1 Equipment

A list of essential laboratory equipment used for the methods of this project includes: the Tecan Safire microplate reader from Tecan Austria GmbH (Austria), The Virtis lyophilizer from Virtis Company (Gardiner, NY), the 96-well Costar plates with UV transparent flat-bottom from Corning, Inc (Corning, NY), the 96-well Costar plates with 2 mL assay block from Corning, Inc (Corning, NY), the Eppendorf Centrifuge 5415 D (Hamburg, Germany), the Harvester96 cell harvester from Tomtec (Hamden, CT), the Jouan C312 Centrifuge (Winchester, VA). Sonifier® Cell disrupter W185 from Heat Systems-Ultrasonics, Inc. (Plainview, LI, NY), the Sonifier® Cell disrupter W350 from Heat Systems-Ultrasonics, Inc. (Plainview, LI, NY), the Wallac 1450 Microbeta® beta counter from PerkinElmer (Waltham, MA), the Axiovert 200M fluorescent microscope from Zeiss (Germany), and the a 460 Watt UV lamp from the University of Massachusetts at Lowell (Lowell, MA).

8.2 Reagents

A list of essential reagents used for the methods of this project includes: beta-glucan particles prepared from Fleishmans Baker's yeast (AB Mauri Food Inc, Chesterfield, MO) according to previously published procedures (Soto and Ostroff, 2008); IgG from sheep IgG purchased from ImmunoReagents, Inc. (Raleigh, NC); Ovalbumin (Ova) from chicken egg white, Ribonucleic acid from torula yeast Type VI (tRNA), chitosan from crab shells, 1,3-diaminopropane (DAP), 25 kDa branched polyethylenimine (PEI), 800 Da linear PEI, hydroxylamine hydroclochloride, ethylenediamine-tetraacetic acid (EDTA), acetic acid, and glycine purchased from Sigma-Aldrich (Allenstown, PA); cell tissue culture materials purchased

from Gibco Scientific (Grand Island, NY); SATA (N-Succinimidyl S-Acetylthioacetate) purchased from Pierce Chemicals (Rockford, IL); thymidine, 1 μCi/well, from PerkinElmer (Boston, MA); 2,2'-dithiolethyl bis(4-azido-2,3,5,6-tetrafluorobenzoate) (DAT) synthesized in the lab of Yan MingDi at UMass Lowell (Lowell, MA); and N-Pyr(Cys) Ova-323-339-amide peptide (ISQAVHAAHAEINEAGR-amide, 90.12% purity) purchased from 21 Century Biochemicals (Marlborough, MA).

9 Methods

All methods represent the final procedures used in completing this project and generating results.

9.1 High-throughput GP protein loading in 96-well plates

9.1.1 Qualitative analysis of 96-well plate loading conditions

Dry empty GP blanks of 5 mg ($2.5x10^9$ particles) were made in a 96-well plate properly sized for a 1 L lyophilization flask. To visualize loading uniformity, varying volumes (10 µL, 20 µL, and 40 µL) of 1 mg/mL Trypan Blue dye in water as were used as a model payload for the primary load. The particles were centrifuged at 1000 rpm for 30 min, frozen to -80ºC, and lyophilized. A water push of varying volumes (5 µL, 10 µL, and 20 µL) was then done to complete the particle loading process. Particles were centrifuged at 1000 rpm for 30 min, frozen to -80ºC, and lyophilized. The effects of primary load volume and water push volume were evaluated by evenness of color in order to determine an ideal high-throughput sequence for loading GPs without hand mixing.

9.1.2 Quantitative analysis of 96-well plate loading conditions

Once ideal volume conditions for dye loading were found, loading of Fluorescein isothiocyanate-labeled Ovalbumin (FL-Ova) through yeast tRNA (yRNA) trapping was examined. Dry GP blanks of 5 mg were made in a 96-well plate properly sized for a 1 L lyophilization tube. Three sets of paired volumes and concentrations (20 µL at 25 mg/mL, 30 µL at 16.7 mg/mL, and 40 µL at 12.5 mg/mL) of FL-Ova were added to individual unloaded GPs to keep the total moles of FL-BSA constant (11.1 nmoles). The plate was centrifuged at 1000 rpm for 30 min, frozen to -

80ºC, and lyophilized. A water push of 20 µL was done and the plate was centrifuged at 1000 rpm for 30 min, frozen to -80ºC, and lyophilized again. The process was repeated using a 10 µL water push. Yeast RNA trapping polymer (2x15 µL at 25 mg/mL) was added to the first set of particles, while saline (2x15 µL) was added to the second set to serve as controls. The plate was centrifuged for 5 min and incubated for 10 min at 50ºC. Yeast RNA (500 µL at 10 mg/mL) was added to the first set, while saline (500 µL) was added to the second control set. All wells were mixed by pipetting and the plate was incubated for 30 min at 50ºC. The plate was then centrifuged at 1000 rpm for 30 min, and the supernatant of each well was transferred to a transparent, 96-well UV plate. MOPS buffer (100 uL, 0.1 M, pH = 7.5) was added to each well of the 96-well UV plate. Fluorescence was read with an excitation wavelength of 494 nm and an emission wavelength of 518 nm. The results of primary load volume versus FL-OVA concentration were evaluated by calculating the average percent loading of each sample (N=3). An identical experiment was done inside tubes for comparison. All loaded GP samples were diluted to 1 mg/mL and imaged under the fluorescent microscope at 100x to assess loading of fluorescent payload.

9.1.3 Macrophage Uptake Microscopy

In order to determine if the particles made in the plate were biologically active, samples loaded with each of three fluorescently labeled proteins (IgG, Lysozyme, and Ovalbumin) inside the 96-well plate were added to a plate of macrophages in media (with a cover slip). Each sample was added to three wells in the macrophage plate. Blank GPs were used as a negative control and GFPs were used as a positive control. After two hours of incubation, the first well of each sample was stopped by removing the cover slip and placing it into a well of a separate plate containing the next well for each sample was stopped at 8 hours and the last at 24 hours. The macrophages were then observed and imaged under the fluorescent microscope at 20x magnification.

9.2 Optimization of GP-NH2 + SATA reaction

9.2.1 Polyamine coupling to GPs through periodate oxidation and borohydride reduction

Dry, empty GPs (10 mg) were suspended in 750 µL water in 15 mL conical tubes. Potassium periodate (0.0043 M) was added to each tube. The mixture was stirred in the dark overnight. The resulting oxidized suspension was centrifuged and the supernatant was discarded. The GPs were washed 3 times with water and suspended in 800 µL water. Borate buffer (200 µL, 0.1 M, pH = 9) was added to each tube and 500 µL of each 5 mg/mL polymer solution (Low MW Chitosan, Linear PEI, and Branched PEI) dissolved in water were added to individual tubes. Low MW Chitosan was dissolved in 0.1 M acetic acid and 500 µL water was added to the control. The particles were suspended and incubated in the dark at room temperature (RT) for 24 hrs. Borate buffer (1 mL, 0.1 M, pH = 9) and 2 mg sodium borohydride (powder) were added to each tube. The samples stirred at RT for 24 hrs and another 2 mg of sodium borohydride (powder) was added to each tube. After all the bubbles had dissipated (over 24 hrs), the samples were washed 8 times with water and suspended in 1 mL saline. The samples were then washed 3 times in water and suspended in 1 mL water at a 10 mg/mL or 5E09 GP/mL particle concentration and stored at -20ºC.

9.2.2 Heparin Assay

Amine-coupled and control GP samples (0.2 mg) were suspended in 100 µL of PBS. Varying amounts of fluorescent rhodamine-heparin in 100 µL of 1X PBS were added to each tube. The samples were incubated for 1 hr at RT. The samples were centrifuged and 100 µL of the

supernatants were transferred to a transparent 96-well UV plate. Fluorescence was measured at an excitation of 540 nm and emission of 577 nm. An EC50 value of the amount of heparin bound to the particles was calculated based on a fluorescent rhodamine-heparin titration curve. The remaining supernatant was discarded, and the samples were washed three times in 1X PBS. The particles were suspended in 1X PBS and imaged using a fluorescent microscope.

9.2.3 SATA binding assay

Amine-coupled GP samples (0.2 mg: Low MW Chitosan, Linear PEI, and Branched PEI) were suspended in 1X PBS. SATA (500 mM) was dissolved in DMSO. Varying amounts of SATA (5 µL, 37µL, and 29 µL) at a 1:1 molar ratio of SATA:amine based on the calculated heparin EC50 binding values were added to each tube, respectively. The samples were incubated for 2 hr at RT in the dark. The samples were then washed three times with water. The supernatants were discarded and the samples were frozen and lyophilized for an Ellman's Assay to measure conjugated thiols.

9.2.4 Ellmans Assay – thiol standard curve

A standard curve of cysteine (100 µL) (0, 0.01875, 0.0375, 0.075, 0.1875, 0.375, and 0.75 µM) in sodium phosphate buffer (0.1 M, pH=8, 1mM EDTA) were made. Sample dilutions (100 µL) in sodium phosphate buffer (0.1 M, pH=8, 1mM EDTA) were made. A solution of Ellman's Reagent (0.01M) in sodium phosphate buffer (0.1 M, pH=8, 1mM EDTA) was made, and 5 µL was added to each sample, excluding the control. The volume of each sample was increased to 200 µL by adding sodium phosphate buffer. After 15 min of incubation in the dark, 100 µL of each sample was placed in a transparent 96-well plate and absorbance was measured at 412 nm. A graph

of absorbance versus moles of cysteine was plotted and an equation was generated for quantifying sulfhydryl groups bound to GPs.

9.2.5 Ellman's Assay of SATA-conjugated samples

A solution of hydroxylamine hydrochloride (HA-HCl) (0.50 M, pH = 7.4, 10 mM EDTA) was prepared in 1X PBS. HA-HCl (5 μL) was added to each 0.2 mg SATA-conjugated GP sample to deprotect the thiol. The samples were sonicated and incubated for 2 hrs in the dark at RT. The samples were then washed three times with 1X PBS. A solution of sodium phosphate buffer (0.1 M, pH = 8, 1 mM EDTA) was prepared. A solution of Ellman's Reagent (0.01 M) in sodium phosphate buffer was made. Ellman's Reagent (5 μL) was added to each deprotected sample. After 15 min of incubation, 195 μL of sodium phosphate buffer was added to each sample. The samples were centrifuged, and 100 μL of supernatant from each tube transferred to a transparent 96-well UV plate. Absorbance was measured at 412 nm, with a reference of 750 nm, and converted into moles of sulfhydryl bound per GP by using the equation of absorbance versus μM cysteine generated from a cysteine standard curve.

9.3 Alternative conjugation approach using DAT

9.3.1 Coupling of DAT to GPs through photoactivation of an aryl azide

Empty, dry GPs (10 mg) were suspended in 2 mL 75% acetone by volume and transferred to dram vials wrapped in aluminum foil. DAT (8 mL, 5.57 mM) in 75% acetone was added to each dram vial. The samples were incubated for 30 min on ice immediately under 450 Watt 280+ nm UV light to avoid light dissipation over distance. The suspensions were collected in microcentrifuge tubes, spun down and the supernatants discarded. Each sample was washed once

in 100% acetone, twice in 75% acetone, and twice in water. The samples were suspended in 1.0 mL saline and 200 μL aliquots were made. The aliquots were centrifuged, the supernatant was discarded, and the tubes were frozen and lyophilized for an Ellman's Assay to measure conjugated thiols.

9.3.2 Ellman's Assay of DAT-conjugated GP samples

A solution of T*ris*(2-carboxyethyl)phosphine (TCEP) (0.125 M, pH = 7.4, 5 mM EDTA) was prepared in 1X PBS.TCEP (10 μL) was added to each 0.2 mg DAT-conjugated GP sample to reduce the thiol. The samples were sonicated and incubated for 2 hrs in the dark at RT. The samples were then washed three times with 1X PBS. A solution of sodium phosphate buffer (0.1 M, pH = 8, 1 mM EDTA) was prepared. A solution of Ellman's Reagent (0.01 M) in sodium phosphate buffer was made. Ellman's Reagent (5 μL) was added to each deprotected sample. After 15 min of incubation, 195 μL of sodium phosphate buffer was added to each sample. The samples were centrifuged, and 100 μL of supernatant from each tube transferred to a transparent 96-well UV plate. Absorbance was measured at 412 nm, with a reference of 750 nm, and converted into moles of sulfhydryl bound per GP by using the equation of absorbance versus μM cysteine generated from a cysteine standard curve.

9.4 Analysis of SATA-conjugated and DAT-conjugated GP samples through N-Pyr(Cys) Ova peptide binding

9.4.1 N-Pyr(Cys) Assay - peptide standard curve

A standard curve of cysteine (100 μL) (0, 0.781, 0.156, 0.3125, 0.625, and 1.25 mM) in water were made. Sample dilutions (100 μL) in were made. A solution of N-Pyr(Cys) Ova peptide

(2.5 mM) in water was made, and 10 μL was added to each sample, excluding the control. The volume of each sample was increased to 200 μL by adding water. After 15 min of incubation in the dark, 200 μL of each sample was placed in a transparent 96-well UV plate and absorbance was measured at 405 nm. A graph of absorbance versus moles of pyridine was plotted and an equation was generated for quantifying Cys Ova peptide bound to GPs.

9.4.2 N-Pyr(Cys) Ova peptide binding assay of SATA-conjugated and DAT-conjugated GP samples

HA-HCl (5 μL) was added to each SATA-conjugated GP sample to deprotect the thiol. TCEP (10 μL) was added to each DAT-conjugated GP sample to reduce the thiol. The GP samples were sonicated and incubated for 2 hrs in the dark at RT. The samples were washed three times with 1X PBS. All samples were suspended in 5 μL of water. N-Pyr(Cys) Ova peptide (5 μL, 2.5 mM) dissolved in water was added to each sample. Duplicates of each sample without addition of N-Pyr(Cys) Ova peptide were included, along with a control of only N-Pyr(Cys) Ova peptide in solution. The samples were incubated for 2 hr in the dark at RT. Water was added to make the final solution volume 200 μL. The samples were centrifuged and the 200 μL of supernatant from each sample was transferred to a transparent 96-well UV plate. Absorbance was read at 405 nm, with a reference of 750 nm. Absorbance was converted into moles of pyridine in solution, which was converted into moles of Cys Ova peptide bound per GP by using the equation of absorbance versus mM pyridine generated from a pyridine standard curve.

9.5 Demonstration of biological utility of GP peptide

9.5.1 OT-II T-cell proliferation assay

Purified T-cells (10^5 cells/well) were incubated with mitomycin C-treated (Bone Marrow Dendritic Cells) BMDCs (10^6 cells/well) and various GP samples for 4 days in round-bottom 96-well plates in 200 µL R10 medium. [^{3}H]-thymidine was added for the last 24 hr of incubation. Each condition of GPs added was studied in triplicate. Cells were collected on filter paper using a harvester, and [^{3}H]-thymidine incorporation was measured with a beta counter (Huang et al., 2010).

10 Results

10.1 High-throughput GP protein loading in 96-well plates

The standard protein loading of GPs requires repetitive mixing steps that make it impractical to produce peptide and protein antigen libraries. Avoiding these mixing steps while maintaining loading efficiency would improve experimental output. Therefore, high throughput methods of loading were tested by loading dyes into GPs in 96-well plates. The distribution of the dyes were examined and evaluated based on evenness of diffusion and deepness of color. Initial experiments used a color change reaction for loading dyes into GPs, but using multiple dyes produced variable results that were difficult to read. The clearest qualitative results were best shown by using a single dye.

Using dyes for loading into GPs allowed for easily visible results showing how well the material spread and diffused throughout the particles without mixing by hand. Plates were prepared with blank GPs and loaded with dye (Figure 2). The plate was then spun in a centrifuge to distribute the dye and allowed to incubate so that the dye diffused throughout the particles. Sets of several wells in the plate were given a different amount of particles and volume of dye in order to determine the ideal amounts. The standard method of loading uses ½ the hydrodynamic volume (20 μL for 5 mg of GPs) of loading material. This experiment was done using ½x hydrodynamic volume (columns 1-4), ¾x hydrodynamic volume (columns 5-8), and 1x hydrodynamic volume (columns 9-12). The plate also contained different amounts of GPs to see if less particles at a time would result in more uniform distribution. Though the ideal size was at least 5mg of particles (rows 1 and 2), amounts of 4 mg (rows 3 and 4), 3 mg (rows 5 and 6), and 2 mg (rows 7 and 8) were also tested. Each well condition had both a hand mixing (odd rows) and non-hand mixing (even rows) counterpart in order to determine if hand mixing significantly affected results.

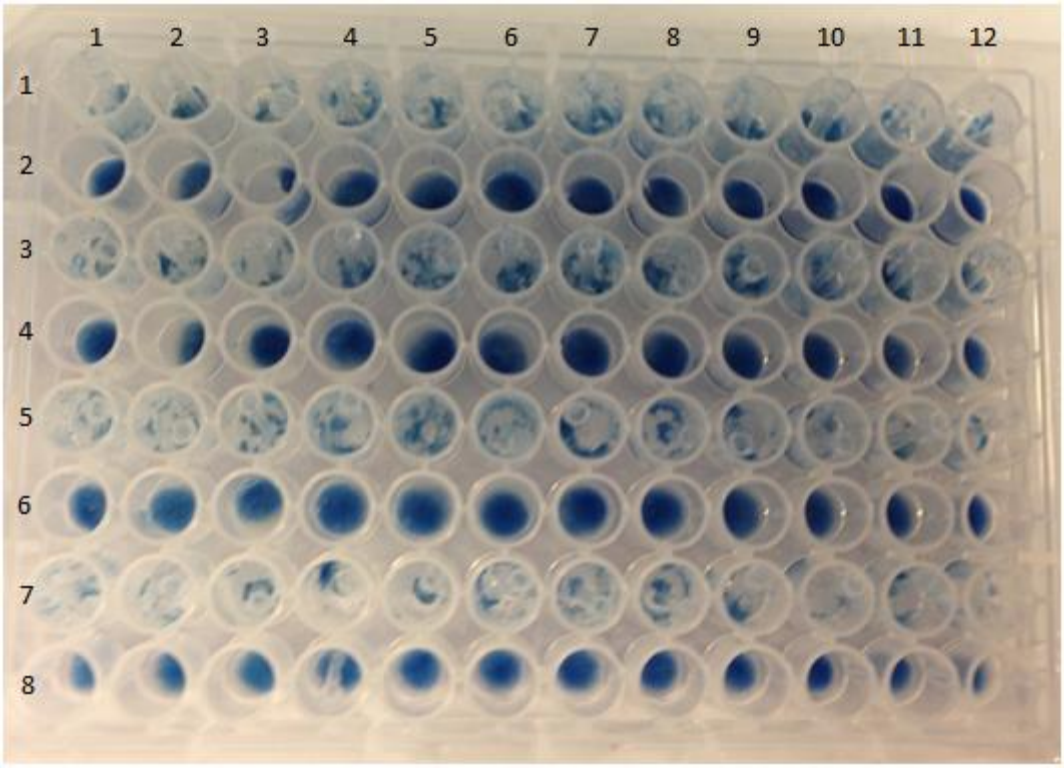

Figure 2: GP Loading with Trypan Blue dye in 96-well plate
Even rows were done with no mixing, Odd rows were done with mixing; Rows 1 & 2 contained 5mg of GPs; Rows 3 & 4 contained 4mg GPs; Rows 5 & 6 contained 3mg of GPs; Rows 7 & 8 contained 2mg GPs; Columns 1-4 contain GPs loaded with 20µL (1/2 the hydrodynamic volume) of 1 mg/mL Trypan Blue dye; Columns 5-8 contain GPs loaded with 30µL (3/4 the hydrodynamic volume) of 1 mg/mL Trypan Blue dye; Columns 9-12 contain GPs loaded with 40µL (1X the hydrodynamic volume) of 1 mg/mL Trypan Blue dye.

The rows in the plate shown in Figure 2 alternated between hand mixing and plate mixing by centrifugation. The mixing wells (rows 1, 3, 5, and 7) did not mix together well, as can be seen by their clumped appearance and by the way the clumps stuck to the sides. The non-mixing wells were much more manageable in the plate. Wells using 1x hydrodynamic volume (columns 9-12) had too much dye and were not practical for use either with or without hand mixing. The remaining wells distributed nicely without having too much remaining liquid. Wells containing 5 mg of particles (rows 1 and 2) showed good distribution of dye even without mixing.

Once the volume of dye that was best for uniform particle loading in a high throughput format was established, this new loading method needed to be quantified in order to determine how effectiveness of GP protein loading in 96-well plates. In order to quantify the efficiency of high throughput GP protein loading without mixing, fluorescent proteins were used. Particles were loaded in 96-well plates using fluorescent lysozyme (14 KDa), Ovalbumin (FL-Ova; 45 kDa) and immunoglobulin (IgG; 150 kDa). The amount of loading in the plate was determined by adding 0.1 M MOPS buffer and measuring unincorporated florescence. The percent loading of FL-Ova in the plate was determined to be 98.78%, the percent loading for Lysozyme was 67.99%, and the percent loading for IgG was 56.46%. The Ova result was compared to the fluorescent reading of particles prepared in tubes, which was 98.83%, by taking the percent difference using the following calculation:

$$\%\, difference = \frac{difference}{average} = \frac{98.83 - 98.78}{\frac{98.83 + 98.78}{2}} = 0.0506\%$$

Plates of particles were set up with 5 mg of GPs per well and loaded with varying volume or concentration of fluorescent proteins to help determine the most effective volume/concentration combination for loading particles in the plate. The loading volumes of fluorescent Ova used were ½x the hydrodynamic volume, ¾x the hydrodynamic volume, and 1x the hydrodynamic volume. The standard method used when loading is done in tubes is ½x the hydrodynamic volume (20 μL for 5 mg of GPs). First wells of ¾x and 1x hydrodynamic volume were loaded using the same concentration of protein as in the ½x hydrodynamic volume but different volumes (30 μL for ¾x and 40 μL for 1x). Next, samples were again made using ¾x and 1x hydrodynamic volume but this time they were done using the same volume (20 μL) as the ½x hydrodynamic volume (this varied concentration). These samples were observed under a fluorescent microscope to look for even loading distribution (Figure 3).

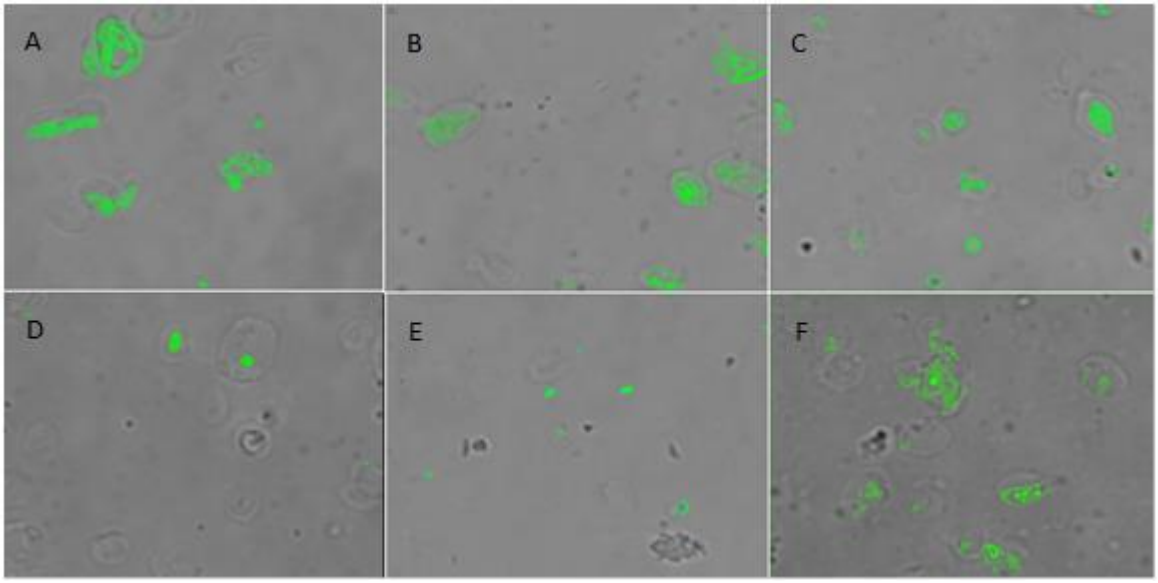

Figure 3: Images of GPs under a fluorescent microscope after loading in a 96-well plate. A) GPs loaded with 20μL (1/2 the hydrodynamic volume) of 25mg/mL Ova and water pushed twice with ¼ hydrodynamic volume with trapper. B) Loaded with 30μL (3/4 the hydrodynamic volume) of 25mg/mL Ova and water pushed once with ½ and once with ¼ hydrodynamic volumes with trapper. C) Loaded with 40μL (1X the hydrodynamic volume) of 25mg/mL Ova and water pushed once with ½ and once with ¼ hydrodynamic volume with trapper. D) Loaded with 30μL of 16.7mg/mL Ova and water pushed once with ½ and once with ¼ hydrodynamic volumes. E) Loaded with 40μL of 12.5mg/mL Ova and water pushed once with ½ and once with ¼ hydrodynamic volumes. F) Control GPs loaded in Tubes

Form observation of the fluorescent protein loaded GPs under the microscope, the 20 μL initial load sample (Figure 3, panel A) had the most even distribution of fluorescent protein trapped inside the GPs, though the 30 μL initial load sample (panel B) also displayed a good distribution. Lower concentrations combined with higher volumes (panels D and E) had much poorer distribution, while higher volume combined with normal concentration (panel C) had a significant amount of trapping outside the GPs.

The samples loaded with each concentration were tested for percent load by adding 0.1 M MOPS buffer and measuring florescence. The percent loaded for the varied concentration are shown in Table 1.

Sample	Loading Volume and Concentration (µL, mg/mL)	Average % Load	Standard Deviation
1	20, 25	95.41	0.86
2	30, 16.7	94.19	0.40
3	40, 12.5	95.60	0.31

Table 1: Average Percent Loaded for Ova in 96-Well Plate

Ideal primary load conditions were established for loading particles in a 96-well plate as ½x hydrodynamic volume with a concentration of 25mg/mL (the same as ideal conditions for tubes). Samples were made using these ideal conditions with three different fluorescent proteins: Ova, lysozyme, and IgG. These samples were added to plates of macrophages and photographed under a fluorescent microscope at 2 hours, 8 hours, and 24 hours in order to determine if the loaded particles were biologically active (Figure 4).

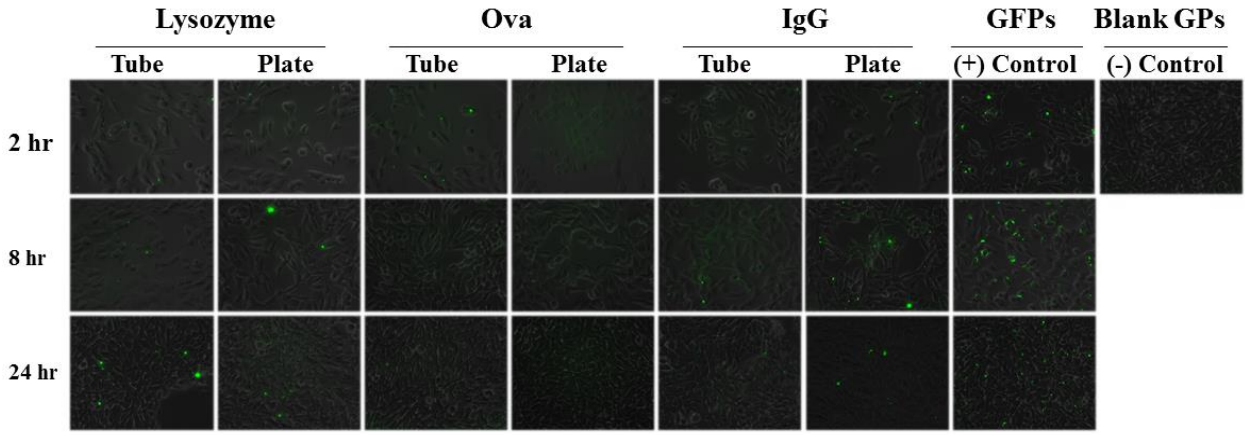

Figure 4: Macrophage Plates of GPs Loaded with Fluorescent Protein in 96-Well Plates vs Traditional Tube Loading
Fluorescent proteins (lysozyme, Ovalbumin, and Immunoglobulin) loaded GPs were added to macrophages. A positive control was included using Green Fluorescent Protein labeled GPs (GFPs) and a negative control was included using blank GPs. Pictures were taken under a fluorescent microscope at 2 hours, 8 hours, and 24 hours.

The cells of the two hour time point contain small fluorescent dots, which are the GPs with fluorescent protein trapped inside them. By the 8 hour mark, the florescence began to spread out inside the cell from fluorescent protein release. This trend continued over the 24 hour period until everything broke down and began dissipating.

10.2 Optimization of GP-NH2 + SATA reaction and alternative conjugation approach using DAT

10.2.1 Evaluation of polyamine-coupled, SATA reacted GPs

In order to continue the testing of binding SATA to amine-derivatized GPs, stocks of amine-coupled GPs were synthesized using adaptations of protocols developed by the Ostroff lab. Five amines were tested: low MW chitosan (~15000 g/mol), linear PEI (25000 g/mol), branched PEI (600 g/mol), DAP (74.12 g/mol), and protamine (5100 g/mol) (Figure 6).

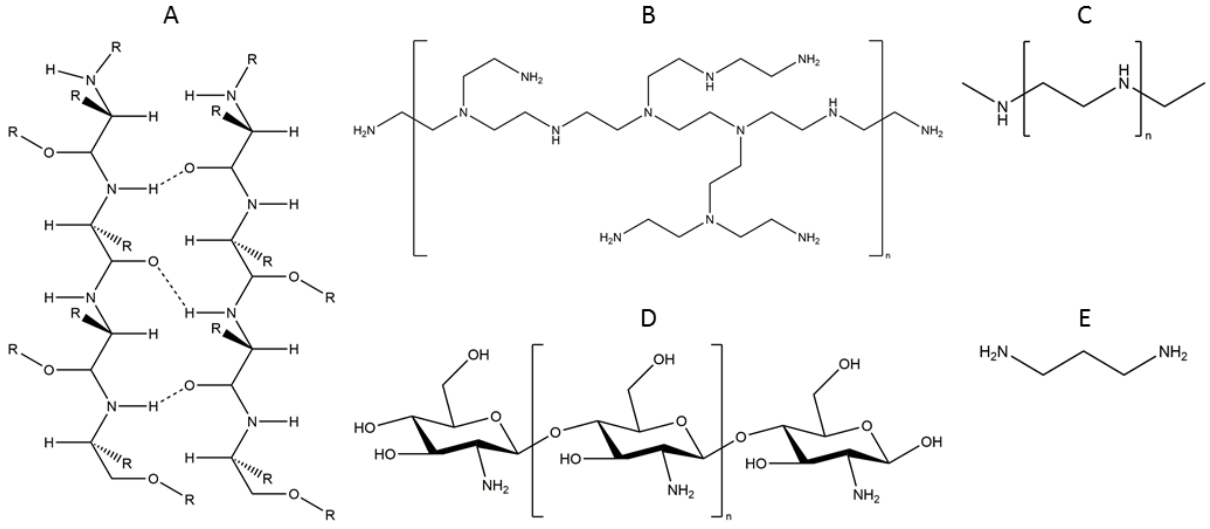

Figure 5: Polyamine chemical structures
(A) The proposed backbone structure of the human protamine-DNA complex (Biegeleisen, 2006). (B) Branched PEI. (C) Linear PEI. (D) Low MW Chitosan. (E) DAP.

In the next coupling experiment, branched PEI and low MW chitosan were examined in place of DAP and protamine. The sodium borohydride reaction time was increased and the reaction was allowed to run to completion. Parafilm was used to cover the tops of the microcentrifuge tubes to prevent bubbling over. However, product was still lost through small "breathing holes" in the Parafilm.

Enough product from each coupling reaction remained for quantification of available surface amine groups through fluorescent heparin binding. Since a Zetasizer could not be used to measure the surface charge of the amine-modified GPs, heparin was used as an indirect measurement of charge. Negatively charged heparin will bind strongly with the positively charged GP surface amine groups. Therefore, measurement of fluorescent heparin remaining in solution gives an indirect measurement of heparin bound to GPs after subtraction from the measured fluorescence of a positive control containing equal, initial unreacted heparin in solution. Each sample was titrated with varying amounts of heparin and fluorescence values of the supernatants were measured (Appendix, Data Table 1). EC50 values were calculated based off the equation generated from the % binding values (Appendix, Data Table 2) plotted in Figure 6.

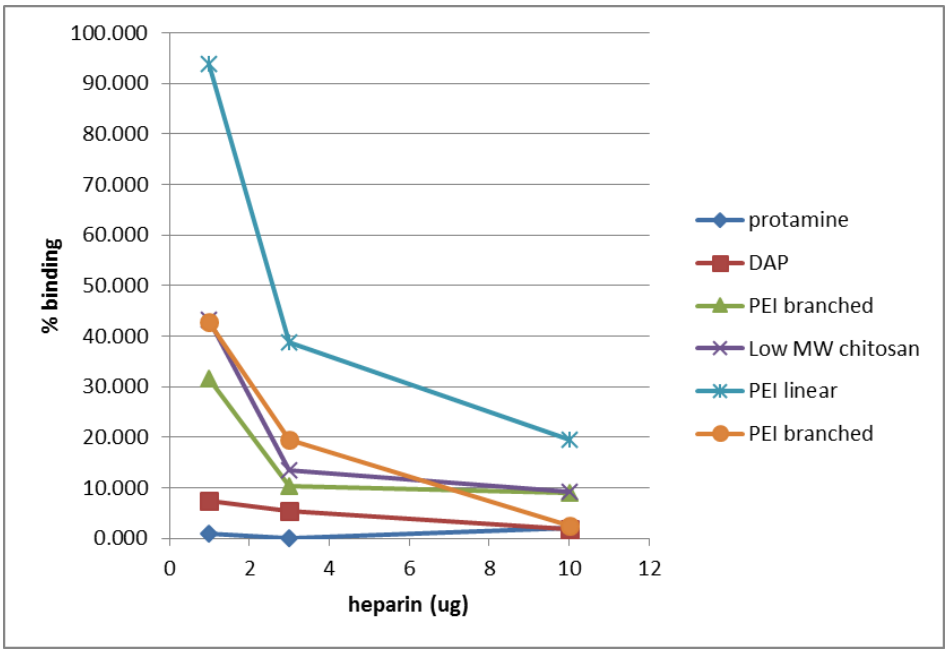

Figure 6: Heparin binding assay of GPs bound with protamine, DAP, branched PEI, linear PEI, and Low MW Chitosan

Polyamine-conjugated GPs were reacted with heparin in solution and fluorescence was measured at an excitation wavelength of 494 nm and an emission wavelength of 519 nm. The amount of fluorescence in solution indirectly correlates with GP surface primary amine residues bound by heparin.

The values showed that GPs modified with linear PEI, low MW chitosan, and branched PEI bound the most heparin and would be predicted to be most reactive with SATA, so these three amine polymers were used to synthesize more stock GPs for further testing. For creating new stocks, 15 mL conical tubes were used in place of 1 mL microcentrifuge tubes. In order to quench the reaction completely, 0.50 mL of glycine was used instead of 0.25 mL. No product was lost due to bubbling.

Heparin binding was, again, used to assess the binding capacity of linear PEI, branched PEI, and low MW chitosan. However, plotted values generated unreadable results, so another assay was done and fluorescence values were measured (Appendix, Data Table 3). The second heparin binding assay with these samples gave measureable results (Figure 7). Linear PEI showed the greatest binding of 65% at 1 µg of heparin added (Appendix, Data Table 4).

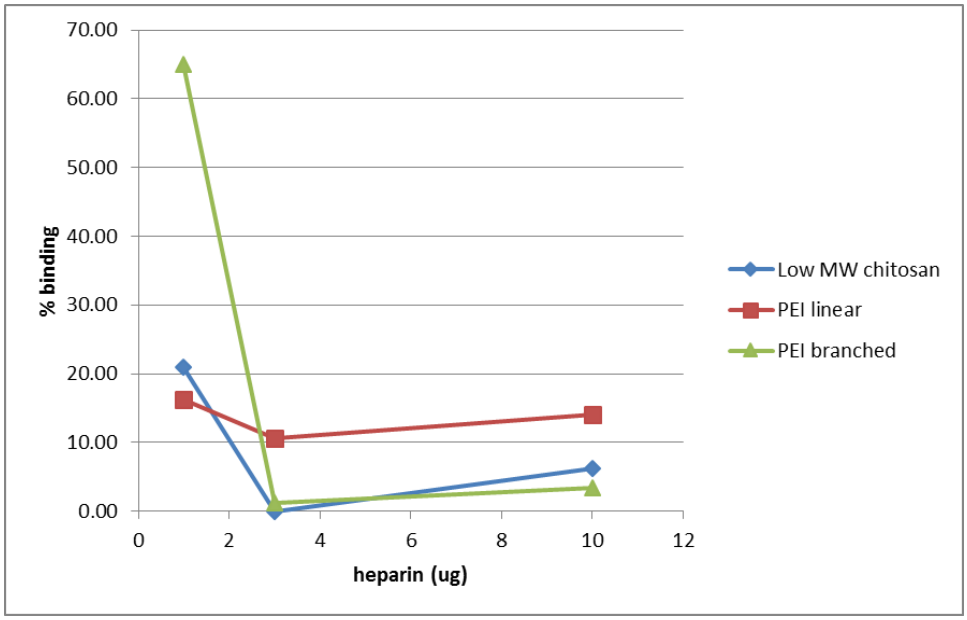

Figure 7: Heparin binding assay of GPs bound with branched PEI, linear PEI, and Low MW Chitosan
Polyamine-conjugated GPs were reacted with heparin in solution and fluorescence was measured at an excitation wavelength of 494 nm and an emission wavelength of 519 nm. The amount of fluorescence in solution indirectly correlates with GP surface primary amine residues bound by heparin.

SATA reaction conditions, including pH and [SATA], were tested and the most reactive GP-amine synthesized compound was chosen through Ellman's Assay (Appendix, Data Tables 5-8). For examining buffer pH, a graph of % binding of each sample versus buffer pH was plotted (Figure 8). Linear PEI showed the only change in moles of sulfhydryl bound with varying buffers. The other samples showed a relatively constant, low output of moles of sulfhydryl bound with

varying buffers (less than 1E-08 moles of thiol per 0.2 mg GPs). Sodium carbonate buffer (0.1 M, pH = 9.2) gave the highest binding with linear PEI (1.47E-08 moles of thiol per 0.2 mg GPs).

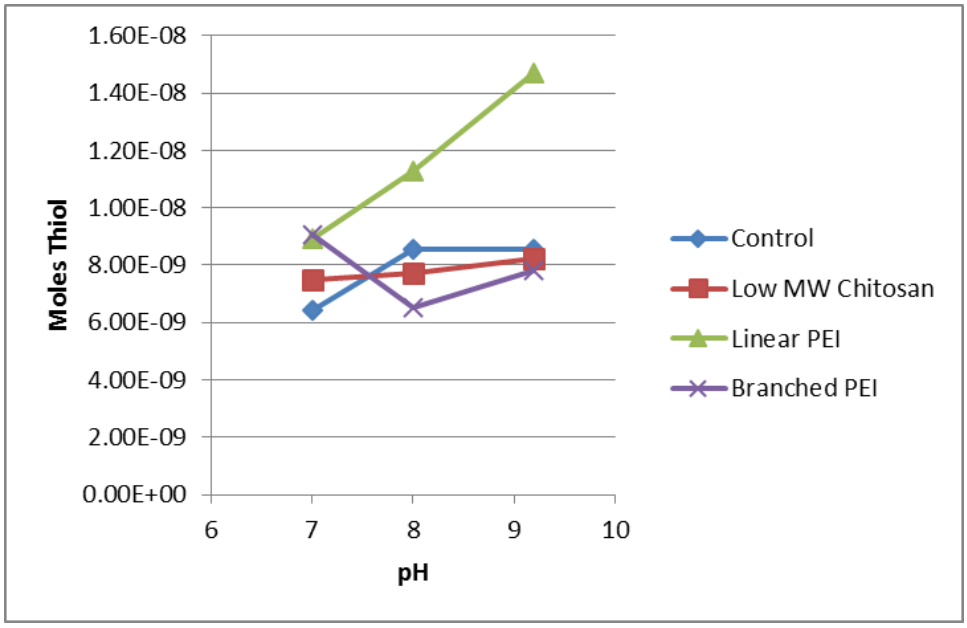

Figure 8: SATA binding assay examining pH=7 and pH=8 phosphate buffer and pH=9.2 sodium carbonate buffer
Polyamine-conjugated GPs were reacted with heparin in solution and fluorescence was measured at an excitation wavelength of 494 nm and an emission wavelength of 519 nm. The amount of fluorescence in solution indirectly correlates with GP surface primary amine residues bound by heparin.

For the following SATA experiment, different concentrations of SATA were examined in pH = 9.2 sodium carbonate buffer. A graph of theoretical moles of sulfhydryl put in versus moles of sulfhydryl out was plotted (Figure 9).SATA reaction increased as the amount of SATA added to each amine-coupled GP sample increased. However, no plateau was shown, indicating that a higher concentration of SATA may be needed in order to completely saturate the coupling reaction.

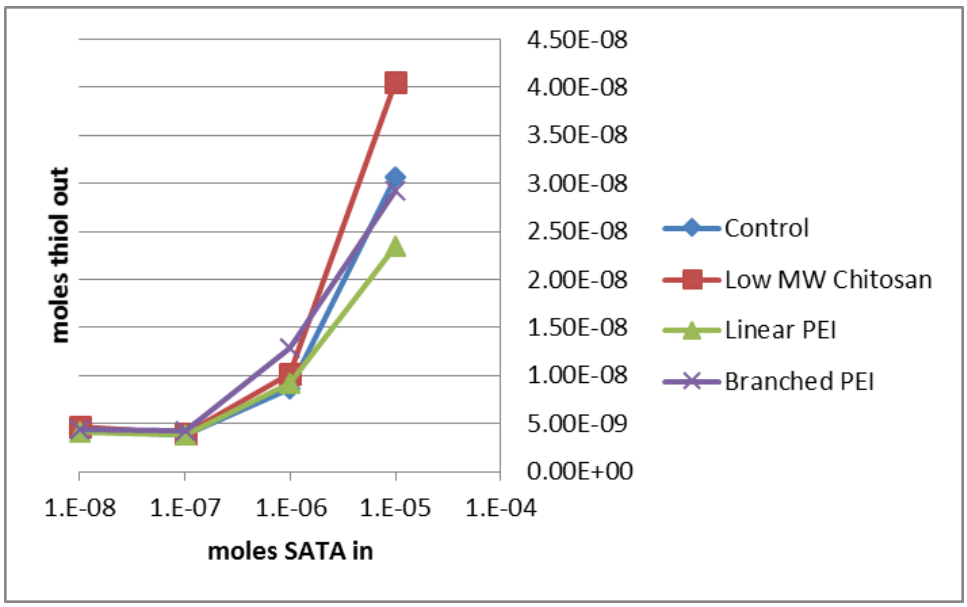

Figure 9: SATA binding assay examining SATA concentration
Polyamine-conjugated GPs were reacted with heparin in solution and fluorescence was measured at an excitation wavelength of 494 nm and an emission wavelength of 519 nm. The amount of fluorescence in solution indirectly correlates with GP surface primary amine residues bound by heparin.

Only linear PEI was used in the following experiment. Since the previous highest concentration of SATA showed no plateau in binding capacity, higher concentrations of SATA were tested (Appendix, Data Tables 9-10). The two highest concentrations of SATA (0.1 M and 0.33 M) displayed a plateau of binding (Figure 10), suggesting that 0.1 M is the highest concentration needed to fully saturate the reductive amination reaction.

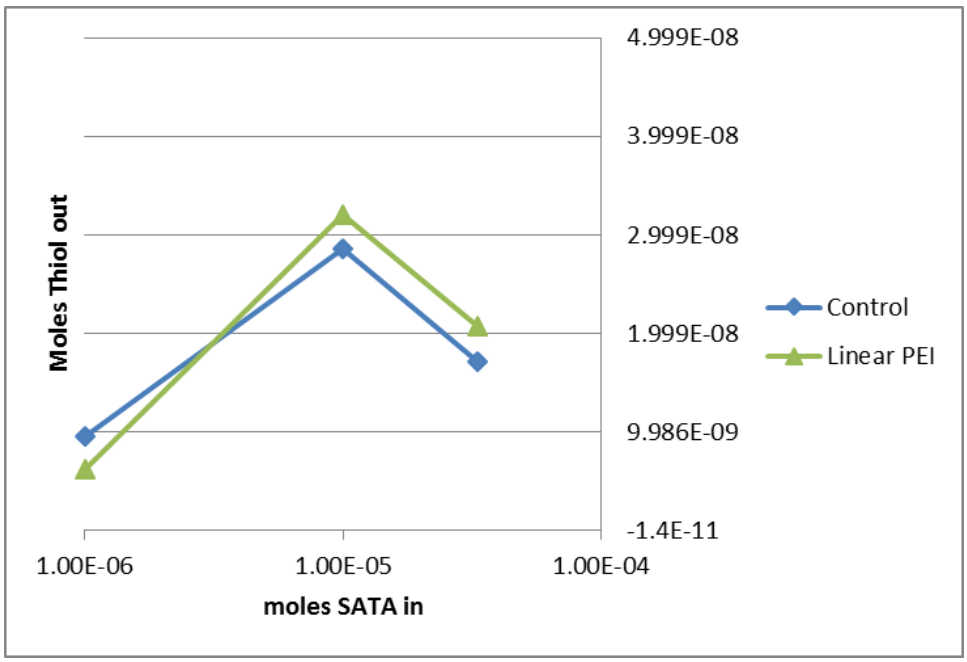

Figure 10: SATA binding assay examining SATA concentration using GPs bound with linear PEI

Linear PEI-conjugated GPs were reacted with heparin in solution and fluorescence was measured at an excitation wavelength of 494 nm and an emission wavelength of 519 nm. The amount of fluorescence in solution indirectly correlates with GP surface primary amine residues bound by heparin.

Since the control GPs showed similar binding to the linear PEI-coupled GPs, another experiment was done to determine if the linear PEI indeed bound to the GPs (Appendix, Data Tables 11-12). Results showed that the linear PEI-coupled GPs bound SATA no more efficiently that control GPs coupled with no amine polymer, suggesting three possibilities (Figure 11): the linear PEI did not bind in the initial reaction, the GPs have uncoupled over time, or the rhodamine-heparin had degraded.

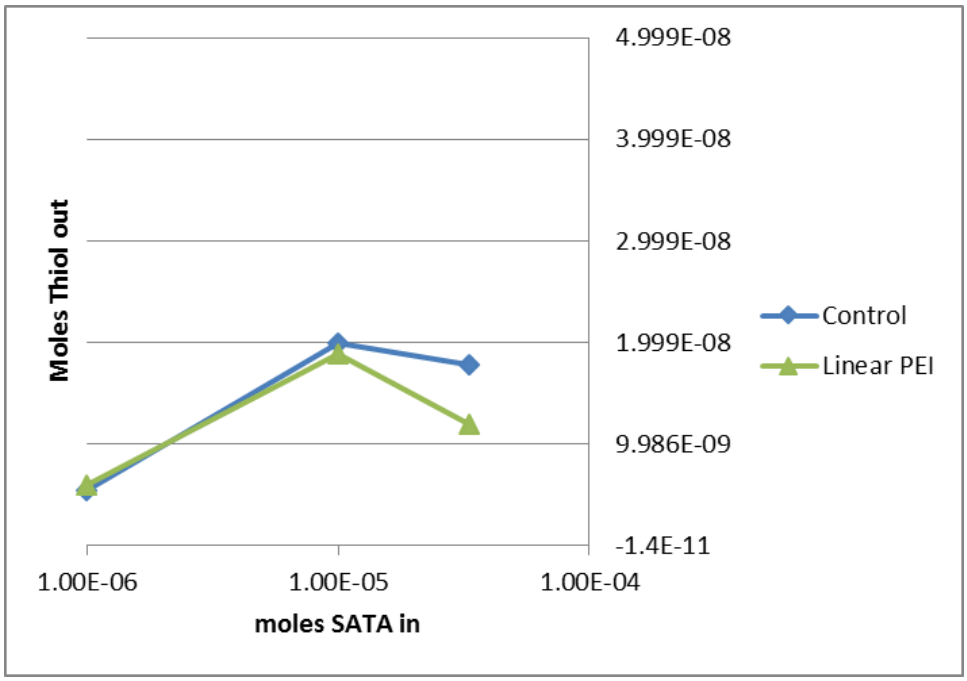

Figure 11: SATA binding assay examining Linear PEI versus blank GPs
Linear PEI-conjugated GPs were reacted with heparin in solution and fluorescence was measured at an excitation wavelength of 494 nm and an emission wavelength of 519 nm. The amount of fluorescence in solution indirectly correlates with GP surface primary amine residues bound by heparin.

The fluorescent labeler, rhodamine-heparan, was tested through a direct reaction with a solution of linear PEI. Solid formation would suggest a working labeler, while no formation of a solid would suggest a degraded fluorescent labeler. The rhodamine-heparin/linear PEI test showed no solid formation, showing that the fluorescent labeler was degraded. A new stock of rhodamine-heparin was made and the heparin binding experiments were repeated (Appendix, Data Tables 13-14). However, similar binding data was gathered and inconsistent results persisted (Figure 12). Therefore, the original amine-coupled GPs were remade using a reductive amination protocol constructed by Jessica Cohen.

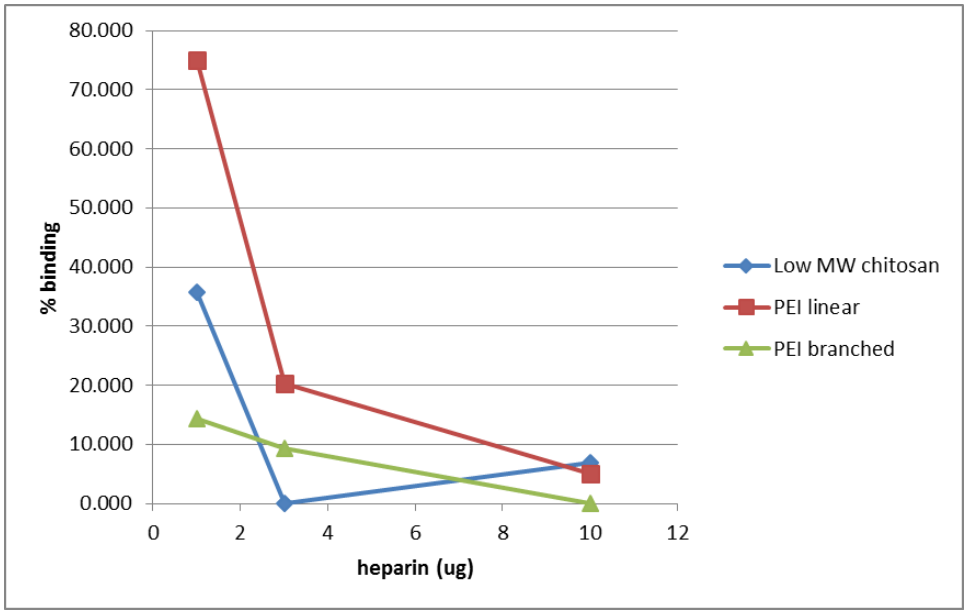

Figure 12: Heparin binding assay reexamining GPs bound with branched PEI, linear PEI, and Low MW Chitosan
Polyamine-conjugated GPs were reacted with heparin in solution and fluorescence was measured at an excitation wavelength of 494 nm and an emission wavelength of 519 nm. The amount of fluorescence in solution indirectly correlates with GP surface primary amine residues bound by heparin.

With slight modifications, the new procedure, outlined in the Methods section, was carried out and new stocks of polyamine-coupled GPs were made. Heparin binding was used to assess the binding capacity of the amine-coupled GPs and calculate EC50 values of each synthesized sample. EC50 values were calculated from the equation generated by the titration curve of % binding values versus log[heparin] (Figure 13). The values showed that Linear PEI GPs (3 112013) and Branched PEI GPs (4 112013) bound heparin efficiently with EC50 values of $3.16 * 10^{-8}$ mol heparin/mg GPs and $2.94 * 10^{-8}$ mol heparin/mg GPs, respectively. Low MW Chitosan GPs (2 112013) bound with an EC50 value of only $5.35 * 10^{-9}$ mol heparin/mg GPs.

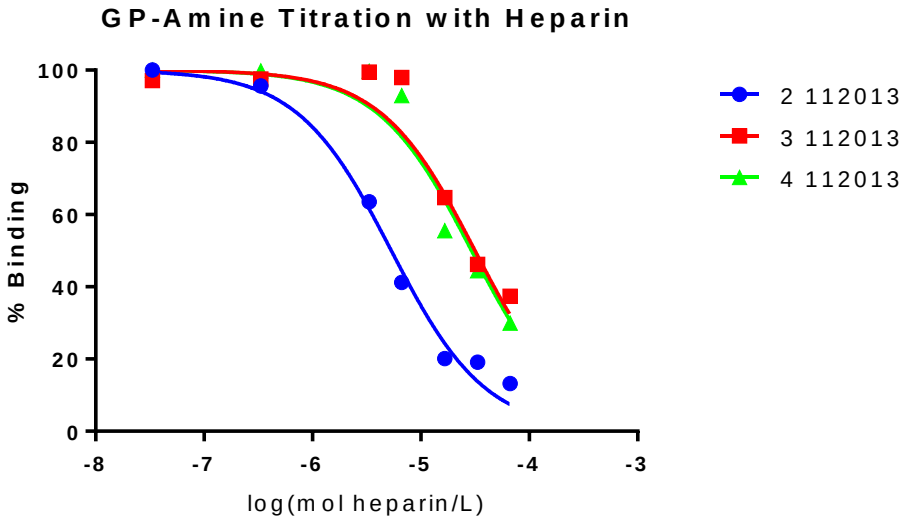

Figure 13: GP-amine titration with heparin
Polyamine-conjugated GPs were reacted with heparin in solution and fluorescence was measured at an excitation wavelength of 494 nm and an emission wavelength of 519 nm. The amount of fluorescence in solution indirectly correlates with GP surface primary amine residues bound by heparin.

The heterobifunctional crosslinker SATA was bound to each newly synthesized polyamine GP sample. Concentration of SATA reacted with each sample was calculated based on previously measured EC50 values from the heparin binding assay. Synthesized amine/SATA GP samples were suspended in saline at 10 mg/mL or 5E09 GP/mL particle concentration and stored at -20ºC for later, final quantification of sulfhydryl groups through Ellman's Assay.

10.3 Alternative conjugation approach using DAT

10.3.1 Evaluation of DAT-coupled GPs

A series of experiments were performed to assess the ability of 2,2'-dithiolethyl bis(4-azido-2,3,5,6-tetrafluorobenzoate to introduce sulfhydryls onto GPs by varying compound concentration and photo-activating light sources. In the first coupling experiment to quantify the

binding capacity of GPs with 2,2'-dithiolethyl bis(4-azido-2,3,5,6-tetrafluorobenzoate), a dilution series of the compound was prepared in 20% DMSO and reacted with GPs under a 15 Watt, 254 nm UV lamp (Appendix, Data Tables 15-19). The distance between the samples and the UV light source was minimized to avoid light intensity dissipation. The modified GPs were reacted with Ellman's Reagent, and the recorded absorbance values reflected a minimal increase in moles of sulfhydryl bound as compound added increased (Figure 14). A duplication of this procedure showed similar low, inconsistent results (Figure 15).

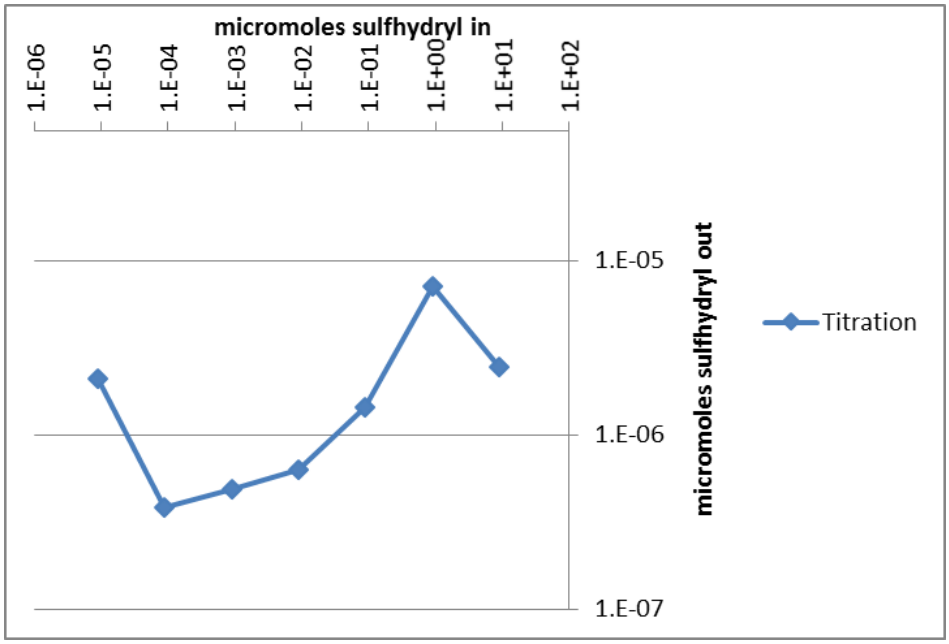

Figure 14: Titration to determine the lowest amount of compound needed to fully couple with a constant amount of GPs (n = 1).
DAT-conjugated GPs subjected to a 15 W, 254 nm UV lamp in 20% DMSO were reacted with Ellman's Reagent and absorbance of TNB^{2-} in solution was measured at a wavelength of 412 nm. The amount of TNB^{2-} in solution directly correlates with GP surface thiol residues displaced by Ellman's Reagent in solution.

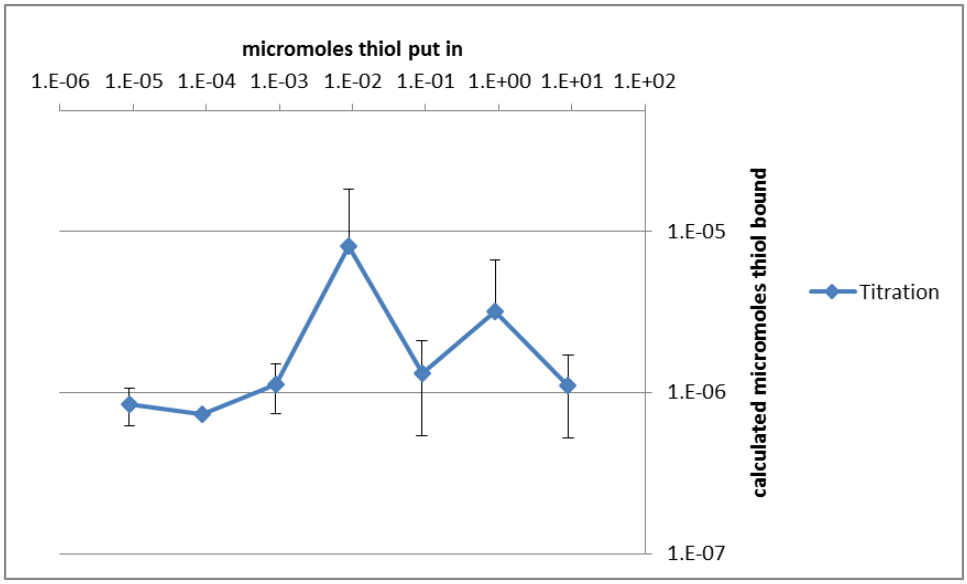

Figure 15: Titration to determine the lowest amount of compound needed to fully couple with a constant amount of GPs (n = 2).
DAT-conjugated GPs subjected to a 15 W, 254 nm UV lamp in 20% DMSO were reacted with Ellman's Reagent and absorbance of TNB^{2-} in solution was measured at a wavelength of 412 nm. The amount of TNB^{2-} in solution directly correlates with GP surface thiol residues displaced by Ellman's Reagent in solution.

Notably, an orange/brown solid was appearing in solution during the photo-activation reaction, so a reaction of only compound in 20% DMSO was carried out (Appendix, Data Table 20). The solid appeared, and the resulting solution was centrifuged and dissolved in DMSO. The solid went back into solution, suggesting it was simply unreacted compound. A white solid material was also seen coming out of solution after addition of the compound to GPs to make a final solution of 20% DMSO. This problem was solved by increasing DMSO concentration until the compound dissolved into solution. A solution of 85% DMSO was necessary to keep 1 mg of DAT dissolved in a 500 μL reaction volume.

A reaction using 85% DMSO was carried out under 15 W, 254 nm UV light (Appendix, Data Tables 21-23). Based on Ellman's assay absorbance, no coupling of DAT to GPs was shown (Figure 16). On average, less than 1E-06 micromoles of thiol bound per 0.2 mg of GPs for any

sample. Therefore, a new light source (copying machine) was used to initiate the reaction (Appendix, Data Tables 24-26). Each sample was flashed 33 times using a copy machine in an attempt to stimulate the reaction to proceed. Ellman's Assay absorbance values gathered from each sample showed no coupling of compound (Figure 17). Only one sample bound higher than 1E-06 micromoles of thiol per 0.2 mg of GPs, but even that value (3.84E-06 micromoles thiol per 0.2 mg GPs) was significantly lower than the theoretical maximum possible moles of thiol bound per mg of GPs using this method (5.55 E-06 moles per 1 mg GPs)

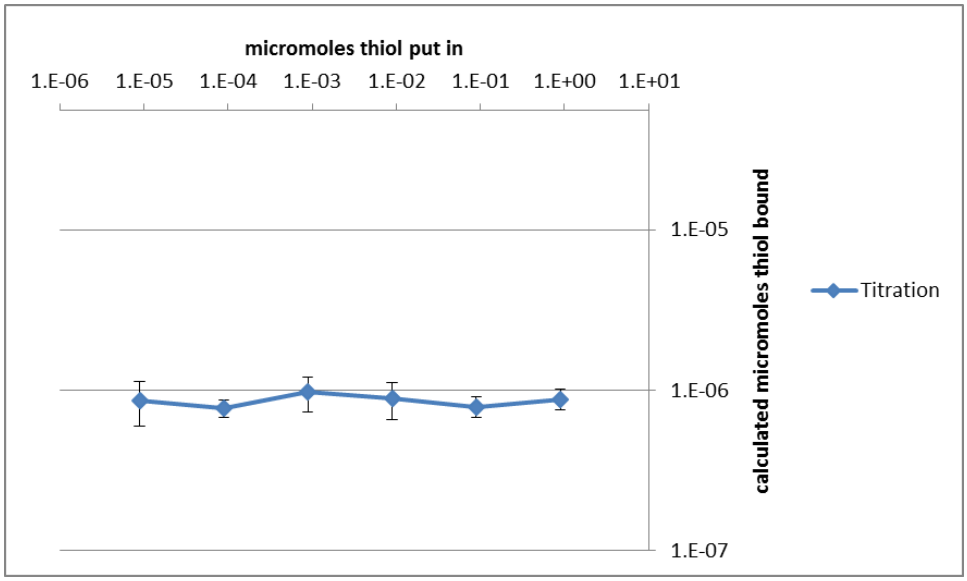

Figure 16: A titration to determine the lowest amount of compound needed to fully couple with a constant amount of GPs (n = 2) in 85% DMSO
DAT-conjugated GPs subjected to a 15 W, 254 nm UV lamp in 85% DMSO were reacted with Ellman's Reagent and absorbance of TNB^{2-} in solution was measured at a wavelength of 412 nm. The amount of TNB^{2-} in solution directly correlates with GP surface thiol residues displaced by cysteine in solution.

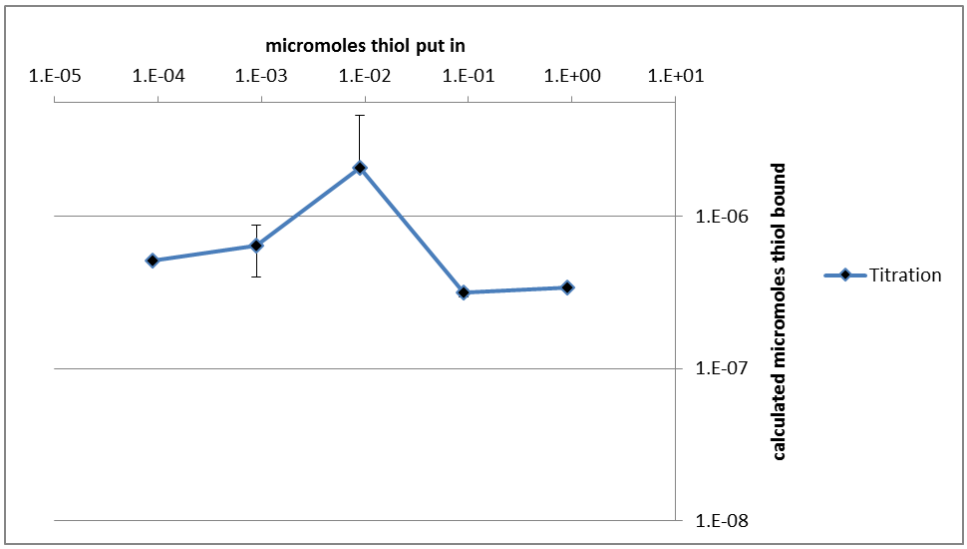

Figure 17: A titration to determine the lowest amount of compound needed to fully couple with a set amount of GPs (n = 2) using a copy machine
DAT-conjugated GPs subjected to a copying machine flash in 85% DMSO were reacted with Ellman's Reagent and absorbance of TNB^{2-} in solution was measured at a wavelength of 412 nm. The amount of TNB^{2-} in solution directly correlates with GP surface thiol residues displaced by Ellman's Reagent in solution.

In an effort to more rapidly initiate the coupling reaction, a 450 W, 280+ nm UV lamp was used as the light source (Appendix, Data Tables 27-28). The reaction was carried out under these new conditions, but Ellman's Assay results proved inconclusive by producing similar results below 1E-06 moles of thiol bound per 0.2 mg of GPs (Figure 18). Therefore, a new solvent was chosen. DAT was dissolved in minimal acetone (75%) and a reaction using the 450 W, 280+ nm UV lamp and a 75% acetone solution was done. Ellman's assay results indicated some binding of sulfhydryl groups (5.81E-06 micromoles of thiol per GP) for the ratio of reacting 1 mg of DAT per 1 mg of particles.

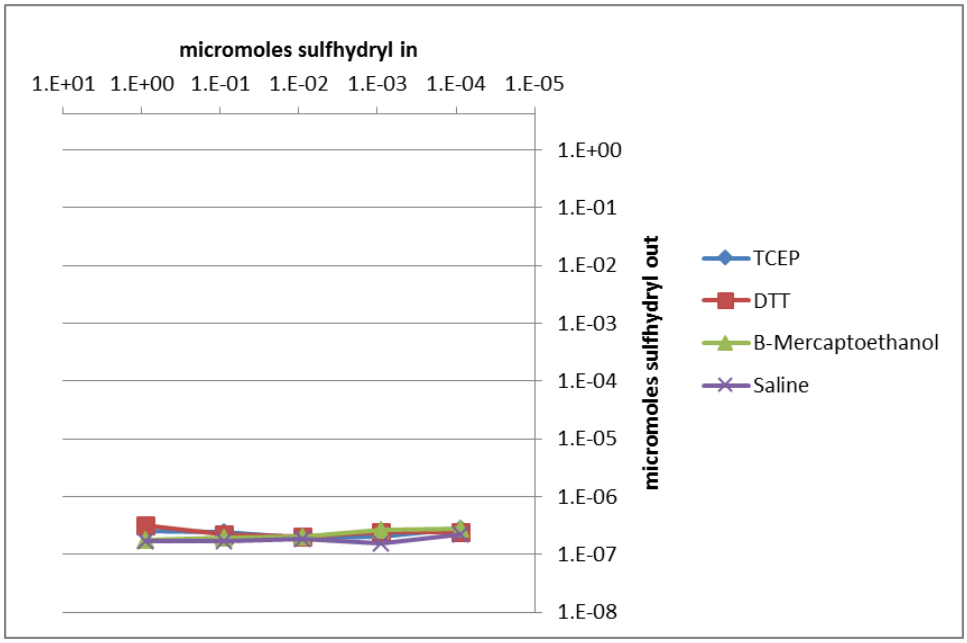

Figure 18: A titration to determine the lowest amount of compound needed to fully couple with a constant amount of GPs while comparing the effects of varying reducing agents on theoretically coupled particles (n = 1)
DAT-conjugated GPs subjected to a 450 W, 280+ nm UV lamp in 75% acetone and were reacted with Ellman's Reagent and absorbance of TNB^{2-} in solution was measured at a wavelength of 412 nm. The amount of TNB^{2-} in solution directly correlates with GP surface thiol residues displaced by Ellman's Reagent in solution.

GPs reacted with DAT were washed with DI water and suspended in saline at 5 mg/mL or 1E09 GP/mL particle concentration, then stored at -20ºC for later, final quantification of sulfhydryl groups through Ellman's Assay.

10.3.2 Ellmans Assay – thiol standard curve

In order to quantify sulfhydryl groups bound to GPs, Ellman's assay with a standard curve using cysteine was created and used (Figure 19).

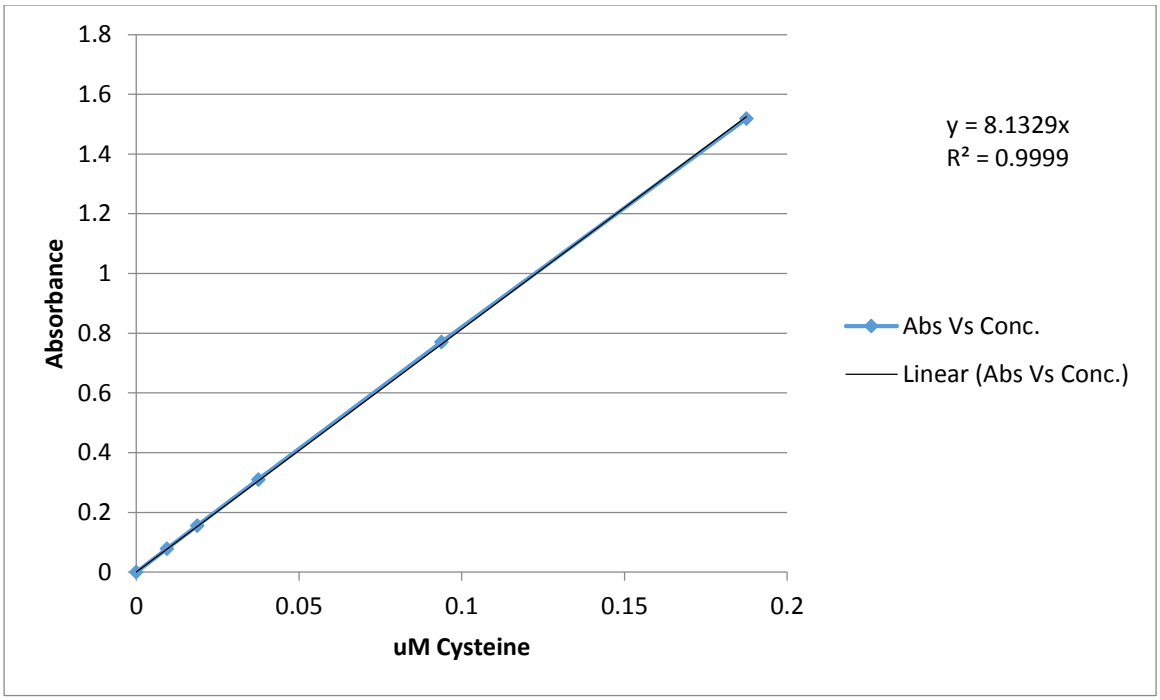

Figure 19: Thiol standard curve for quantification of free sulfhydryl groups
A set standard of cysteine solutions were made and reacted with Ellman's Reagent. Absorbance of TNB^{2-} in solution was measured at a wavelength of 412 nm. The amount of TNB^{2-} in solution directly correlates with thiol residues displaced by Ellman's Reagent in solution.

The recorded absorbance directly corresponded with moles of sulfhydryl bound by Ellman's Reagent within the linear range (A ~0.01 - 2). The standard curve gave the equation and R^2 value:

$$Absorbance = 8.1329 * \mu M\ Cysteine$$

$$R^2 = 0.9999$$

The cysteine standard established through Ellman's assay was used to convert all Ellman's assay results of modified particles into free moles of thiol per GP.

10.3.3 Ellman's Assay of SATA-conjugated and DAT-conjugated GP samples

With polyamine/SATA-conjugated and DAT-conjugated particles successfully made, Ellman's assay was used to quantify the number of available thiol groups for each sample (Table 2). Measurement of TNB^{2-} in solution from Ellman's assay revealed that DAT-coupled GPs bound more Ellman's Reagent (molecules of Ellman's Reagent = molecules of thiol) per GP than Low MW Chitosan-coupled GPs. However, both Linear PEI-coupled GPs and Branched PEI-coupled GPs bound more Ellman's Reagent per mg of GPs than DAT-coupled GPs.

Derivatization	Molecules of thiol per GP
DAT	6926
Low MW Chitosan-SATA	2931
Linear PEI-SATA	59260
Branched PEI-SATA	70230

Table 2: Summary of SATA-GP and DAT-GP Ellman's Assay

10.3.4 N-Pyr(Cys) Assay – Cys-containing peptide standard curve

In order to quantify the amount of N-Pyr(Cys) peptide bound to GPs, a standard curve binding cysteine with free peptide was created (Figure 20). Free peptide in solution was bound to varying concentrations of free cysteine to create a linear plot of absorbance versus concentration of pyridine.

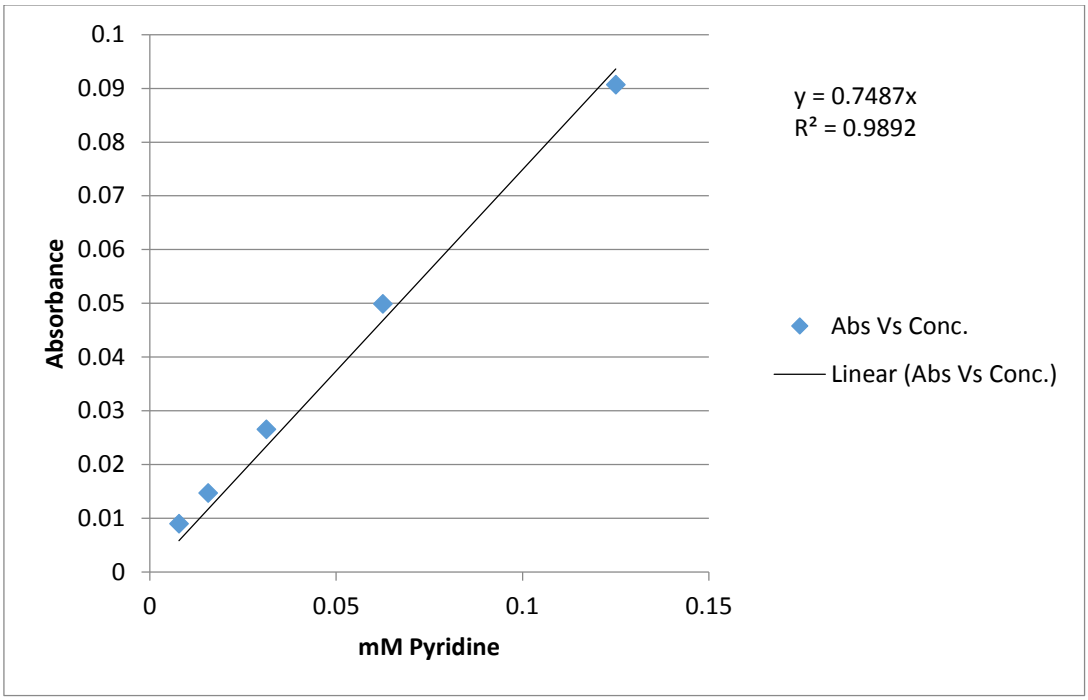

Figure 20: N-Pyr(Cys) peptide standard for quantification of active thiol groups
A set standard of cysteine solutions were made and reacted with free N-Pyr(Cys) Ova peptide. Absorbance of pyridine in solution was measured at a wavelength of 405 nm. The amount of pyridine in solution directly correlates with thiol residues displaced by cysteine in solution.

Measurement of pyridine concentration directly represented the amount of peptide bound by cysteine within the linear range (A ~0.01 - 2). The standard curve gave the equation and R^2 value:

$$Absorbance = 0.7487 * \text{mM Pyridine}$$

$$R^2 = 0.9892$$

The pyridine standard was used to convert all N-Pyr(Cys) Ova peptide binding assay absorbance results into moles of peptide bound per GP.

10.3.5 N-Pyr(Cys) Ova peptide binding assay of SATA-conjugated and DAT-conjugated GP samples

N-Pyr(Cys) peptides selectively react with free thiol groups, forming disulfide bonds. This covalent linkage creates a protected sulfhydryl group that prevents peptide S-S dimers from forming. The N-terminal pyridine broken off into solution provides a colored reaction product to measure direct peptide conjugation efficiency at 405 nm. Analysis of N-Pyr(Cys) Ova peptide binding to SATA-conjugated and DAT-conjugated GP samples revealed that SATA-derivatized GPs bound Cys-containing peptides more efficiently than DAT-derivatized GPs (Table 3).

GP Type	mol Pyr/mg GP
DAT GPs	$1.215 * 10^{-8}$
Linear PEI-SATA GPs	$1.897 * 10^{-8}$

Table 3: N-Pyr(Cys) Ova peptide binding results

However, in comparison with the Ellman's assay results quantifying free thiol groups, DAT used 6 times more available thiols to bind the N-Pyr(Cys) Ova peptide, suggesting that DAT-modified GPs bind and then release Cys peptide more efficiently than SATA-modified GPs.

10.4 Demonstration of biological utility of GP peptide

10.4.1 OT-II cell proliferation assay

In order to demonstrate whether N-Pyr(Cys) Ova peptide-encapsulated GPs and Ovalbumin-loaded GPs can effectively deliver antigen to T-cells, an *in vitro* [3H]-thymidine T-cell proliferation assay was performed (Figure 7). CD4+ T-cells obtained from OT-II mice were stimulated *in vitro* with GPs bound with N-Pyr(Cys) Ova peptide and GPs loaded with Ovalbumin. The results indicated that DAT surface-derivatized GP-N-Pyr(Cys) led to an enhanced CD4+ T-cell proliferation, compared to polymer/SATA-derivatized GPs (30000 CPM compared to 8000

CPM). This assay demonstrated that the N-Pyr(Cys) peptide was delivered, processed, and presented by dendritic cells more efficiently with DAT-bound GPs than with polymer/SATA-bound GPs.

For GP loaded Ovalbumin samples, the plate-loaded samples showed the same biological activity as the tube-loaded samples (50000-70000 CPM), suggesting that high-throughput GP loading in 96-well plates using Ovalbumin is as efficient a method as the standard GP loading procedure. In addition, GPs loaded with lysozyme/BSA stimulated a minimal cell response in both the 96-well plate and the tube (~8000 CPM). However, GPs loaded with IgG/BSA did stimulate T-cell proliferation (60000-70000 CPM), suggesting that there is some other factor allowing IgG to stimulate OT-II T-cell response.

Tube	Name
1	Saline
2	conA
3	Blank GPs
4	Ova 1, Plate/Tube
5	Ova 1, Tube
6	Ova 2, Tube
7	Ova 3, Tube
8	Ova 1, Plate
9	Ova 2, Plate
10	Ova 3, Plate
11	Lys, Tube
12	Lys, Plate
13	IgG, Tube
14	IgG, Plate
15	Ova 2, DAT/SATA
16	DAT, Ova
17	DAT, control
18	SATA, Ova
19	SATA, control

Table 4: OT-II T-cell Legend

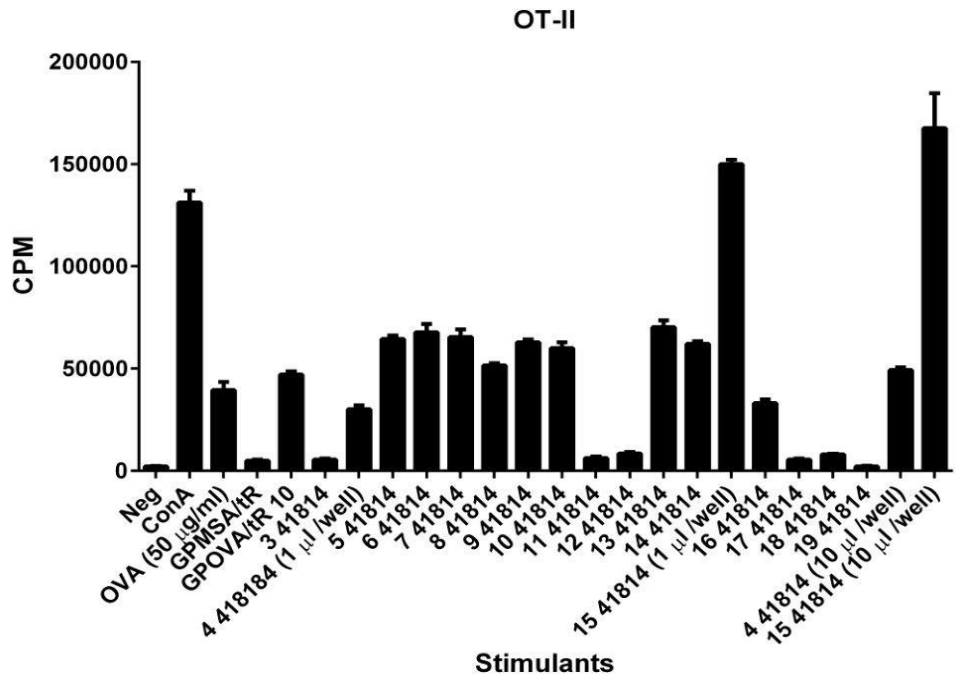

Figure 21: OT-II T-cell proliferation assay of loaded and bound GPs
A [^{3}H]-thymidine T-cell incorporation assay was performed by stimulating OT-II T-cells using compounds listed in Table 4. Results for were measured using Wallac 1450 Microbeta® beta counter in counts per minute (CPM) and the CPM values were plotted.

11 Discussion

11.1 High-throughput GP protein loading in 96-well plates

The current method for loading GPs involves tedious hand mixing and waiting in between steps. If loading could be done without mixing, then this process could be done in a 96-well plate. In order to determine if mixing by hand is necessary, GPs were loaded with dye inside of a 96-well plate. This experiment involved testing several loading volumes and each variable combination was tested with hand mixing and without. Figure 2 shows that the Trypan Blue dye distributed relatively evenly without hand mixing. Some wells had more dye then necessary, so those loading volumes were ruled out for later experimentation. The volume that appeared to distribute well enough for further testing were ½x the hydrodynamic volume of the particles, which is the amount used for standard protein loading into particles using the original tube loading method. Using ¾x and 1x the hydrodynamic volume also appeared to distribute evenly, so these volumes were examined further.

The dye experiments allowed for a rough visual estimate of which loading volumes were most effective in the plate, but the dye was not able to give quantitative results. Therefore, further experiments using fluorescent proteins were necessary. GPs were loaded with the original ½x hydrodynamic volume as well as with ¾x and 1x the hydrodynamic volume. These two loading volumes were done both by varying the overall volume added as well as by varying the concentration but not the volume. Figure 3 shows images of these fluorescent particles under the microscope. From the figure, the particles clearly contained fluorescence, which visibly demonstrates that the loading worked. Comparing the different loading variations under the microscope led to the conclusion that the original ½x loading volume achieves the best distribution

in the plate. This conclusion is based on the even distribution of fluorescence among GPs in the samples examined under the fluorescent microscope.

To further support this conclusion, fluorescence readings were taken after adding 0.1 M MOPS buffer to the samples to make the resulting pH = 7.4. This pH balance allowed for a quantitative analysis of the amount of fluorescence present in the particles. Table 1 clearly shows the difference in loading amount between the different loading volumes. This table also shows that both the original ½x and the 1x hydrodynamic volumes produce over 95% loading in the plate loading format. Though the 1x hydrodynamic volume produced a slightly higher percent loading, there was more fluorescence shown to be trapped outside of the particles when examined under the microscope. Therefore, using ½x the hydrodynamic volume for the initial protein load is still a better option for loading particles in the plate. The percent loaded into the GPs in the plate is definitely high enough to utilize a 96-well plate format a viable high-throughput option.

After establishing that using a 96-well plate is a feasible GP loading method, the loading of different-sized protein molecules was examined. The three proteins which we tested loading for were: Ovalbumin (45 kDa), Lysozyme (15 kDa), and IgG (150 kDa). The results showed that only Ovalbumin loaded with high efficiency (98.78%), while the percent loading for Lysozyme was 67.99% and the percent loading for IgG was 56.46%. Lysozyme and IgG may not have loaded efficiently due to size restrictions. Lysozyme is a small protein in comparison to Ova, so diffusion into and out of the particles may have occurred more freely, balancing the equilibrium. With a balanced equilibrium, the concentration of lysozyme outside of the particles would be equal to the concentration inside of the particles, so when subjected to yeast tRNA trapping, efficiency would be shown to be around 50%. As for IgG, the larger size may have made diffusion into the particles more difficult. If mixed more vigorously or for a longer period of time, more IgG molecules may

have entered the GPs, giving a higher loading efficiency. Besides size restrictions, the lysozyme may have loaded less efficiently in comparison to Ova due to the use of (Bovine Serum Albumin) BSA as a conjugate matrix in the lysozyme and IgG samples. Ovalbumin forms a matrix with yeast tRNA, trapping both inside the GPs. However, lysozyme and IgG do not form a matrix with yeast tRNA, so BSA was mixed in and used as a substitute for matrix formation. The addition of BSA to lysozyme and IgG may have given an unfavorable interaction that decreased the percent loading of both compounds into the particles. Overall, IgG and lysozyme were not shown to load efficiently into GPs, whereas Ovalbumin did load efficiently.

The final step to determining if GPs can be loaded efficiently in a 96-well plate was to show that the loaded particles were biologically active. This goal was accomplished by adding three GP samples loaded with fluorescent proteins (FL-Ova, FL-lysozyme, and FL-IgG) to macrophage cells and examining uptake. Figure 3 shows that, after 2 hour incubation, the macrophages ingested the GPs, shown as a small fluorescent punctate. After 8 hours, the particles began to break down and the fluorescent contents spread throughout the cell. By 24 hours the fluorescence began to dissipate. The appearance of fluorescence between samples varied due to the use of different fluorescent labels. Ovalbumin was labeled using fluorescein isothiocyanate (FITC), while IgG and lysozyme were labeled using Alexa-Fluor 488 dye, which produced a significantly stronger response to excitation and emission at wavelengths 495 nm and 519 nm, respectively. Therefore, IgG-loaded and lysozyme-loaded GPs appeared brighter than Ova-loaded GPs under a fluorescent microscope at 20x. The eventual diffusion and fading of the fluorescence in the cells showed that the particles were biologically active and that loading in a 96-well plate produced bioactive GPs.

11.2 Optimization of GP-NH2 + SATA reaction and alternative conjugation approach using DAT

Methods for binding cysteine-containing peptides to GPs have been previously developed by the Ostroff lab using the heterobifunctional crosslinker SATA. The process of reductive amination links amine-containing polymers to the surface aldehydes of periodate oxidized GPs. The subsequent reaction of SATA with amine-coupled GPs yields terminal sulfhydryl groups used for cysteine-containing peptide linkage through disulfide bonds. Previous attempts at this peptide coupling method worked but amines unreacted with SATA led to ionic interactions between acidic cysteine-containing peptides and the polyamines on the surface of the particles (Negmetzhanov, 2012). A salt wash work around was developed to release any peptide bound by ionic interactions, but this method decreases the efficiency of the overall reaction. Methods to avoid these ionic interactions were sought but none proved successful. Ionic interactions seemed to have remained even in final N-Pyr(Cys) binding reactions, which produced un-cleavable peptide. Although the SATA GPs bound more peptide than DAT GPs, T-cell response was minimal, which was indicative of biologically inactive ionically bound peptide. Altering pH, buffers, and concentrations of reactants had minimal effect on altering overall SATA reaction efficiency. However, the polyamines linear PEI and branched PEI both gave higher binding efficiency than low MW chitosan, which was the polymer of choice in previously defined procedures. The heparin binding assay showed that linear PEI GPs and branched PEI GPs bound heparin efficiently with EC50 values of $3.16 * 10^{-8}$ mol heparin/mg GPs and $2.94 * 10^{-8}$ mol heparin/mg GPs, respectively, while low MW Chitosan GPs only bound with an EC50 value of only $5.35 * 10^{-9}$ mol heparin/mg GPs. In the future, a smaller primary amine linker for GP and SATA could be examined. Linear PEI, with a compact, linear structure, showed great peptide binding results and may have shown efficient biological activity as well if used instead of branched PEI. Branched PEI, with a bulky

structure, bound peptide well but most likely contained interfering charged amine residues decreasing biological activity. A short, low MW (<600 Da), linear polyamine may produce fewer charged, free amine groups and would not be sterically problematic for SATA linking.

To overcome the limitations of the SATA coupling approach a novel process for linking cysteine-containing peptides to the surface of GPs was pursued. Similar to reductive amination, nitrene chemistry was used in an attempt to directly link a sulfhydryl-containing compound to the surface of the GPs. By using a powerful, low wavelength UV lamp, the azide group of the compound DAT could be broken down into a nitrene, which reacts with C-H groups on the outside of the GP shell (Hermanson, 1996). This covalent bond would produce a reducible sulfhydryl bond in the center of the bound compound, similar to the SATA linkage. The overall reaction time is 30 minutes, while the combined reaction times for the polyamine/SATA method is over 3 days for creation of free sulfhydryl groups. Therefore, this new reaction would offer the same result in significantly less time. However, results showed that using the DAT compound gave 10-fold less free, active thiol groups per particle than did the SATA compounds. Ellman's Assay used to measure incorporated thiol onto the branched PEI-labeled SATA particles showed $7.10 * 10^4$ molecules of thiol bound per GP, while DAT particles showed $7.00 * 10^3$ molecules of thiol bound per GP.

After creating free sulfhydryl groups on the surface of GPs, biological activity of the particles is examined through the binding of cysteine-containing peptides. N-Pyr(Cys) Ova peptide ligates with sulfhydryl groups, knocking off one pyridine molecule per peptide into solution. The concentration of these pyridine molecules can be read by measuring absorbance at 405 nm. The results showed that the DAT-modified GPs bound fewer moles of peptide per GP than did the SATA-modified GPs. However, using the measured value of free sulfhydryl groups from Ellman's

assay, the DAT-modified GPs bound peptide to a higher percentage of free sulfhydryl groups than did the SATA-modified GPs. This disparity in peptide binding efficiency suggests there is some factor decreasing overall reaction efficiency for SATA-modified GPs in comparison to DAT-modified GPs. Steric hindrance of the polyamine structure of branched PEI, which was the polymer tested through N-Pyr(Cys) Ova binding, may prevent peptide in solution from binding completely or ionic interactions between the N-Pyr(Cys) Ova peptide and polyamine/SATA-modified GPs may prevent bound peptide from breaking off into solution.

11.3 Demonstration of biological utility of GP peptide

The unique structure of GPs allowed recognition and uptake by phagocytic dendritic cells or macrophages (APCs; antigen presenting cells) from OVA transgenic T-cell receptor (TCR) mice. The CD4+ OT-II T cells in these mice specifically recognize Ova peptide, allowing for extremely efficient Ova protein digestion into Ova peptide presentation by APCs. The MHC-II Ova antigens presented to CD4+ OT-II T cells stimulated cellular proliferation measured using a [^{3}H]-thymidine T-cell proliferation assay (Huang et al., 2010). GPs containing surface-linked Ova N-Pyr(Cys) peptide samples and GPs containing core loaded Ova protein samples were co-cultured with APCs and CD4+ OT-II T cells to assess proliferation. OT-II T cell proliferation was assessed by [^{3}H]-thymidine incorporation. Both N-Pyr(Cys) Ova-peptide derivatized GPs and Ova protein-loaded GPs stimulated CD4+ T-cell proliferation. Specifically, the high-throughput method of loading Ova protein in 96-well plates proved equally successful in comparison to Ova loaded into GPs using the standard technique. Both plate-loaded and tube-loaded Ova GPs saw upwards of 70000 CPM, indicating excellent OT-II T-cell responses due to effective antigen processing and presentation by APCs. Lysozyme-loaded GP samples did not induce an OT-II T-

cell response due to the absence of a reactive epitope. However, IgG-loaded GPs did produce a T-cell response. The IgG compound may have formed a bioactive matrix with the BSA loading substitute, although unlikely. The IgG contained trace amounts of sheep serum albumin, but a cross-reactive response for OT-II T cells recognizing the Ova epitope was unlikely. During synthesis of the GP Ova, GP IgG, GP lysozyme, Ovalbumin may have cross-contaminated with the IgG samples, but this possibility is questionable because the lysozyme samples would have likely become contaminated as well. SDS PAGE analysis of the loaded GP vaccines could probe for extra bands of contaminant. If Ovalbumin were trapped in the IgG sample matrix, then a band would show at 45 kDa, the MW of Ovalbumin. Other than some unlikely method of contamination, no obvious explanations can be determined immediately. Other methods of loading IgG in GPs should be examined to discover the biological properties of loading IgG in GPs. These properties could elucidate any possible explanations for the stimulated OT-II T-cell immune response from GPs loaded with IgG.

DAT modified GPs produced a stronger OT-II T cell response than branched PEI/SATA modified GPs. The assay showed that the N-Pyr(Cys) Ova peptide encapsulated on surface-modified GPs using the novel compound DAT stimulated stronger Ova-specific T-cell proliferation *in vitro* compared to SATA-modified GPs despite SATA having shown 10-fold more binding through Ellman's Assay. One factor influencing biological activity of each modified GP type may be structural capacity. DAT is a small compound in comparison to an amine polymer, and direct linkage of DAT to the surface of GPs yields limited steric hindrance. Large amine polymers bound to the GP surface provide steric hindrance for subsequent binding assays, and since derivatization using polyamines also requires SATA linkage, the efficiency of the succeeding peptide binding may be severely limited. In addition, if any amine groups remain unreacted, then

the possibility of ionic interactions yielding un-cleavable peptide by glutathione greatly increases. The methods using the novel compound DAT for binding peptides onto the surface of GPs for the purpose of vaccine delivery should be pursued and optimized to greater enhance DAT conjugation so that antigen delivery and presentation through peptide binding is maximized.

12 Conclusions and Recommendations

High-throughput protein loading methods of GPs were established for 96-well plates and found to have equal biological activity using a macrophage uptake assay as compared to standard tube GP protein loading format. Functional testing of loaded GPs using murine transgenic OT-II T-cells confirmed the utility of the GP-loaded proteins for vaccine delivery *in vitro*. Next steps are to test vaccines *in vivo* and use this method to prepare a GP antigen protein library. Multi-step GP derivatization with cationic amine polymers followed by reaction with SATA gave higher GP Cys-peptide binding efficiencies than the one-step direct reaction between GPs and the novel compound DAT. However, functional testing of loaded GPs using murine transgenic OT-II T-cells showed that the GP/DAT-linked peptides stimulated a stronger T-cell response than the GP/SATA-linked peptides *in vitro*. Future work should consist of evaluating reaction conditions to enhance the coupling of DAT to GPs; alternate solvents and buffer solutions should be considered to increase coupling efficiency.

13 Bibliography

Akira S and Hemmi H. (2003). Recognition of pathogen-associated molecular patterns by TLR family. *Immunology Letters*, *85*, 85-95.

Biegeleisen, Ken. (2006). The probable structure of the protamine–DNA complex. *Journal of theoretical biology*, *241.3*: 533-540.

Brown G and Gordon S. (2001). Immune recognition: a new receptor for B-glucans. *Nature, 413*: 36-37.

Clark A, Kerrigan A, and Brown G. (2011). *Biology and chemistry of beta glucan*. 1: 19-20. SAIF Zone, Sharjah, UAE: Bentham Science Publishers.

Hermanson, Greg T. (1996). Light sources and conditions for photoactivation of aryl azide crosslinking and labeling reagents. *Bioconjugate Techniques, 1st Edition*. Pierce Biotechnology, Rockford, IL.

Huang H, Ostroff GR, Lee CK, Specht CA, and Levitz SM. (2010). Robust stimulation of humoral and cellular immune responses following vaccination with antigen loaded-glucan particles. *MBio, 1*: e00164-10.

LaRosa D, and Orange J. (2008). Lymphocytes. *Journal of Allergy and Clinical Immunology*. *121*: S364-S369.

Negmetzhanov, B. (2012). Beta-glucan particles as a delivery system in peptide vaccine development. Informally published manuscript, Biology, Worcester Polytechnic Institute, Worcester, MA.

Ohana T, Shimoyama M, Niino, H, and Yabe A. (1995). Excimer-laser-induced polymerization of diazido compounds. *Journal of Photochemistry and Photobiology A: Chemistry*, *87*, 61-65.

Riedel, S. (2005). Edward Jenner and the history of smallpox and vaccination. *Baylor University Medical Center Proceedings*, *18*, 21-25.

Sanders L and Hendren R. (1997). Vaccine Design. *Protein Delivery Physical Systems*. Hingham, Ma: Kluwer Academic Publishers.

Soto E and Ostroff G. (2008). Characterization of Multilayered Nanoparticles Inside Yeast Cell Wall Particles for DNA Delivery. *Bioconjugate Chemistry, 19*, 840-848.

Soto E, Kim YS, Lee J, Kornfeld H, and Ostroff G. (2010). Glucan particle encapsulated rifampicin for targeted delivery to macrophages. *Polymers, 2*: 681–689.

Soto ER, Caras AC, Kut LC, Castle MK, and Ostroff GR. (2011). Glucan Particles for Macrophage Targeted Delivery of Nanoparticles. *Journal of Drug Delivery, vol. 2012*, ID 143524, 13.

Yan J, Allendorf D, and Brandley B. (2005). Yeast whole glucan particle (WGP) β-glucan in conjunction with antitumour monoclonal antibodies to treat cancer. *Expert Opinions on Biological Therapies*, *5*: 691-702.

14 Appendix

Data Table 1: 5/29/2013, Heparin binding assay fluorescence readings

Description	GP (mg)	Heparin (µg)	Fluorescence
Heparin Control	0	0	0
Heparin Control	0	1	5428
Heparin Control	0	3.3	16250
Heparin Control	0	10	47128
Blank GPs	0.02	0	16
Blank GPs	0.02	1	7600
Blank GPs	0.02	3.3	15659
Blank GPs	0.02	10	45529
1 51513	0.02	1	4363
2 51513	0.02	1	4318
3 51513	0.02	1	4043
4 51513	0.02	1	2981
1 52013	0.02	1	11733
2 52013	0.02	1	6661
3 52013	0.02	1	711
4 52013	0.02	1	6706
1 51513	0.02	3.3	44628
2 51513	0.02	3.3	47658
3 51513	0.02	3.3	42241
4 51513	0.02	3.3	40045
1 52013	0.02	3.3	43772
2 52013	0.02	3.3	37910
3 52013	0.02	3.3	26792
4 52013	0.02	3.3	35200
1 51513	0.02	10	46750
2 51513	0.02	10	45827
3 51513	0.02	10	45933
4 51513	0.02	10	42494
1 52013	0.02	10	42083
2 52013	0.02	10	38163
3 52013	0.02	10	33884
4 52013	0.02	10	41043

Data Table 2: 5/29/2013, Heparin binding assay EC50 values

Description	1 µg	3 µg	10 µg	EC50 (ug heparin)	EC50 (mol heparin)
2 51513	1.031	0	1.974	28.744	1.916E-09
3 51513	7.334	5.349	1.748	0.0577	3.849E-12
4 51513	31.675	10.269	9.104	0.301	2.005E-11
2 52013	43.229	13.392	9.315	0.873	5.818E-11
3 52013	93.940	38.792	19.483	2.357	1.572E-10
4 52013	42.845	19.583	2.471	1.038	6.923E-11

Data Table 3: 6/21/2013, Heparin binding assay fluorescence readings

Name	GP (mg)	Heparin (µg)	Fluorescence
Heparin Control	0	0	0
Heparin Control	0	1	3024
Heparin Control	0	3.3	15513
Heparin Control	0	10	40313
Blank GPs	0.02	0	7
Blank GPs	0.02	1	4397
Blank GPs	0.02	3.3	17162
Blank GPs	0.02	10	47482
1 61013	0.02	1	4659
2 61013	0.02	1	3686
3 61013	0.02	1	3898
4 61013	0.02	1	1630
5 61013	0.02	3.3	16569
6 61013	0.02	3.3	16670
7 61013	0.02	3.3	14813
8 61013	0.02	3.3	16362
9 61013	0.02	10	46683
10 61013	0.02	10	43804
11 61013	0.02	10	40115
12 61013	0.02	10	45096

Data Table 4: 6/21/2013, Heparin binding assay EC50 values

Description	1	3	10	EC50 (µg heparin)	EC50 (mol heparin)
2 62113	20.88	0	6.17	-	-
3 62113	16.33	10.60	14.07	-	-
4 62113	65.01	1.249	3.40	1.323	8.82E-11

Data Table 5: 6/28/2013, SATA binding protocol examining buffer pH description

Old Tube	New Tube	Description	GP-polymer (mg)	pH buffer	[SATA] (M)
1 61013	1 62813	Control	0.2	7 phos.	0.01
2 61013	2 62813	Low MW Chitosan	0.2	7 phos.	0.01
3 61013	3 62813	Linear PEI	0.2	7 phos.	0.01
4 61013	4 62813	Branched PEI	0.2	7 phos.	0.01
1 61013	5 62813	Control	0.2	8 phos.	0.01
2 61013	6 62813	Low MW Chitosan	0.2	8 phos.	0.01
3 61013	7 62813	Linear PEI	0.2	8 phos.	0.01
4 61013	8 62813	Branched PEI	0.2	8 phos.	0.01
1 61013	9 62813	Control	0.2	9.2 carb.	0.01
2 61013	10 62813	Low MW Chitosan	0.2	9.2 carb.	0.01
3 61013	11 62813	Linear PEI	0.2	9.2 carb.	0.01
4 61013	12 62813	Branched PEI	0.2	9.2 carb.	0.01
	-	Blank	0	-	0
	-	Blank w/Ellman's	0	-	0

Data Table 6: 6/28/2013, SATA binding protocol examining buffer pH absorbance readings

Description	Absorbance	Moles out	Moles in
Control	0.0514	6.43E-09	1.00E-06
Low MW Chitosan	0.06	7.50E-09	1.00E-06
Linear PEI	0.0713	8.91E-09	1.00E-06
Branched PEI	0.0726	9.08E-09	1.00E-06
Control	0.0685	8.56E-09	1.00E-06
Low MW Chitosan	0.0616	7.70E-09	1.00E-06
Linear PEI	0.0901	1.13E-08	1.00E-06
Branched PEI	0.0523	6.54E-09	1.00E-06
Control	0.0685	8.56E-09	1.00E-06
Low MW Chitosan	0.0657	8.21E-09	1.00E-06
Linear PEI	0.1176	1.47E-08	1.00E-06
Branched PEI	0.0625	7.81E-09	1.00E-06
Blank	0	0	0
Blank w/Ellman's	0.0403	5.04E-09	0

Data Table 7: 7/01/2013, SATA binding protocol examining SATA concentration description

Old Tube	New Tube	Description	GP-polymer (mg)	pH buffer	[SATA] (M)
1 61013	1 70113	Control	0.2	9.2 carb.	0.1
2 61013	2 70113	Low MW Chitosan	0.2	9.2 carb.	0.1
3 61013	3 70113	Linear PEI	0.2	9.2 carb.	0.1
4 61013	4 70113	Branched PEI	0.2	9.2 carb.	0.1
1 61013	5 70113	Control	0.2	9.2 carb.	0.01
2 61013	6 70113	Low MW Chitosan	0.2	9.2 carb.	0.01
3 61013	7 70113	Linear PEI	0.2	9.2 carb.	0.01
4 61013	8 70113	Branched PEI	0.2	9.2 carb.	0.01
1 61013	9 70113	Control	0.2	9.2 carb.	0.001
2 61013	10 70113	Low MW Chitosan	0.2	9.2 carb.	0.001
3 61013	11 70113	Linear PEI	0.2	9.2 carb.	0.001
4 61013	12 70113	Branched PEI	0.2	9.2 carb.	0.001
1 61013	13 70113	Control	0.2	9.2 carb.	0.0001
2 61013	14 70113	Low MW Chitosan	0.2	9.2 carb.	0.0001
3 61013	15 70113	Linear PEI	0.2	9.2 carb.	0.0001
4 61013	16 70113	Branched PEI	0.2	9.2 carb.	0.0001
	-	Blank	0	-	0
	-	Blank w/Ellman's	0	-	0

Data Table 8: 7/01/2013, SATA binding protocol examining [SATA] absorbance readings

Description	Absorbance	Moles out	Moles in
Control	0.2454	3.07E-08	0.00001
Low MW Chitosan	0.3248	4.06E-08	0.00001
Linear PEI	0.1874	2.34E-08	0.00001
Branched PEI	0.2342	2.93E-08	0.00001
Control	0.0688	8.60E-09	0.000001
Low MW Chitosan	0.0819	1.02E-08	0.000001
Linear PEI	0.0735	9.19E-09	0.000001
Branched PEI	0.1027	1.28E-08	0.000001
Control	0.031	3.88E-09	0.0000001
Low MW Chitosan	0.0318	4.00E-09	0.0000001
Linear PEI	0.0303	3.79E-09	0.0000001
Branched PEI	0.0345	4.31E-09	0.0000001
Control	0.0335	4.19E-09	0.00000001
Low MW Chitosan	0.0369	4.61E-09	0.00000001
Linear PEI	0.0324	4.05E-09	0.00000001
Branched PEI	0.0349	4.36E-09	0.00000001
Blank	0	0	0
Blank w/Ellman's	0.0338	4.23E-09	0

Data Table 9: 7/08/2013, SATA binding protocol examining SATA concentration description

Old Tube	New Tube	Description	GP-polymer (mg)	pH buffer	[SATA] (M)
1 61013	1 70813	control	0.2	9.2 carb.	0.33
3 61013	2 70813	Linear PEI	0.2	9.2 carb.	0.33
1 61013	3 70813	control	0.2	9.2 carb.	0.1
3 61013	4 70813	Linear PEI	0.2	9.2 carb.	0.1
1 61013	5 70813	control	0.2	9.2 carb.	0.01
3 61013	6 70813	Linear PEI	0.2	9.2 carb.	0.01
	-	Blank	0	-	0
	-	Blank w/Ellman's	0	-	0

Data Table 10: 7/08/2013, SATA binding protocol examining [SATA] absorbance readings

Description	Absorbance	Moles out	Moles in
control	0.1373	1.716E-08	0.000033
Linear PEI	0.1653	2.066E-08	0.000033
control	0.2284	2.855E-08	0.00001
Linear PEI	0.2558	3.198E-08	0.00001
control	0.0761	9.513E-09	0.000001
Linear PEI	0.049	6.125E-09	0.000001
Blank	0	0	0
Blank w/Ellman's	0.0288	3.6E-09	0

Data Table 11: 7/30/2013, SATA binding protocol examining SATA concentration description

Old Tube	New Tube	Description	GP-polymer (mg)	pH buffer	[SATA] (M)
1 61013	1 73013	Control	0.2	9.2 carb.	0.33
3 61013	2 73013	Linear PEI	0.2	9.2 carb.	0.33
1 61013	3 73013	Control	0.2	9.2 carb.	0.1
3 61013	4 73013	Linear PEI	0.2	9.2 carb.	0.1
1 61013	5 73013	Control	0.2	9.2 carb.	0.01
3 61013	6 73013	Linear PEI	0.2	9.2 carb.	0.01
	-	Blank	0	-	0
	-	Blank w/Ellman's	0	-	0

Data Table 12: 7/30/2013, SATA binding protocol examining [SATA] absorbance readings

Description	Absorbance	moles Out	Moles in
Control	0.1417	1.771E-08	0.000033
Linear PEI	0.0949	1.186E-08	0.000033
Control	0.159	1.988E-08	0.00001
Linear PEI	0.1504	1.88E-08	0.00001
Control	0.0426	5.325E-09	0.000001
Linear PEI	0.0472	5.9E-09	0.000001
Blank	0.0001	1.25E-11	0
Blank w/Ellman's	0.0282	3.525E-09	0

Data Table 13: 7/26/2013, Heparin binding assay fluorescence readings

Tube	Description	GP (mg)	Heparin (µg)	Fluorescence
1 62113	Heparin Control	0	0	0
2 62113	Heparin Control	0	1	2782
3 62113	Heparin Control	0	3.3	12806
4 62113	Heparin Control	0	10	47539
5 62113	Blank GPs	0.02	0	-14
6 62113	Blank GPs	0.02	1	4435
7 62113	Blank GPs	0.02	3.3	15710
8 62113	Blank GPs	0.02	10	49324
9 62113	1 61013	0.02	1	4327
10 62113	2 61013	0.02	1	2781
11 62113	3 61013	0.02	1	1085
12 62113	4 61013	0.02	1	3709
13 62113	1 61013	0.02	3.3	15237
14 62113	2 61013	0.02	3.3	15230
15 62113	3 61013	0.02	3.3	12140
16 62113	4 61013	0.02	3.3	13810
17 62113	1 61013	0.02	10	47575
18 62113	2 61013	0.02	10	44323
19 62113	3 61013	0.02	10	45215
20 62113	4 61013	0.02	10	47726

Data Table 14: 7/26/2013Heparin binding assay EC50 values

Tube	1 µg	3 µg	10 µg	EC50 (µg heparin)	EC50 (mol heparin)	µg SATA per 0.2 mg GP	Mol SATA per 0.2 mg GP
2 62113	35.729	0.0459	6.836	9.738	6.49E-10	97.38	4.21E-07
3 62113	74.925	20.326	4.961	2.173	1.45E-10	36.21	1.57E-07
4 62113	14.282	9.365	0	0.0340	2.26E-12	0.0136	5.88E-11

Data Table 15: 6/05/2013, GP titration with DAT description

Old Tube	New Tube	Description	GP (mg)	DAT (µg)
	1 60613	Just buffer	0	0
	2 60613	Just Ellman's and buffer	0	0
2 60513	3 60613	No DAT	0.2	0
2 60513	4 60613	No DAT - reduced	0.2	0
3 60513	5 60613	sample	0.2	2000
4 60513	6 60613	sample	0.2	200
5 60513	7 60613	sample	0.2	20
6 60513	8 60613	sample	0.2	2
7 60513	9 60613	sample	0.2	0.2
8 60513	10 60613	sample	0.2	0.02
9 60513	11 60613	sample	0.2	0.002

Data Table 16: 6/05/2013, GP Titration with DAT absorbance readings

Description	Absorbance	Calc. mol per well	Total µmol out	µmol put in
Just buffer	0			
Just Ellman's and buffer	0.0444	1.41E-13		
No DAT	0.047	1.67E-13		
No DAT - reduced	0.0875	5.72E-13		
sample	0.1528	1.225E-12	0.00000245	8.918219923
sample	0.3855	3.552E-12	0.000007104	0.891821992
sample	0.1021	7.18E-13	0.000001436	0.089182199
sample	0.0619	3.16E-13	0.000000632	0.00891822
sample	0.0547	2.44E-13	0.000000488	0.000891822
sample	0.0495	1.92E-13	0.000000384	8.91822E-05
sample	0.1346	1.043E-12	0.000002086	8.91822E-06

Data Table 17: 6/10/2013, GP titration with DAT description

Old Tube	New Tube	Description	GP (mg)	DAT (µg)
	1 61013	Just buffer	0	0
	2 61013	Just Ellman's and buffer	0	0
	3 61013	No DAT	0.2	0
	4 61013	No DAT - reduced	0.2	0
3 60513	5 61013	sample	0.2	2000
4 60513	6 61013	sample	0.2	200
5 60513	7 61013	sample	0.2	20
6 60513	8 61013	sample	0.2	2
7 60513	9 61013	sample	0.2	0.2
8 60513	10 61013	sample	0.2	0.02
9 60513	11 61013	sample	0.2	0.002
	12 61013	No DAT	0.2	0
	13 61013	No DAT - reduced	0.2	0
3 60513	14 61013	sample	0.2	2000
4 60513	15 61013	sample	0.2	200
5 60513	16 61013	sample	0.2	20
6 60513	17 61013	sample	0.2	2
7 60513	18 61013	sample	0.2	0.2
8 60513	19 61013	sample	0.2	0.02
9 60513	20 61013	sample	0.2	0.002

Data Table 18: 6/10/2013, GP titration with DAT absorbance readings

Description	Absorbance	Calc. mol per well	Total µmol out	µmol put in
Just buffer	0			
Just Ellman's and buffer	0.056	2.57E-13		
No DAT	0.0836	5.33E-13		
No DAT - reduced	0.8454	8.151E-12		
sample	0.1068	7.65E-13	0.00000153	8.918219923
sample	0.3111	2.808E-12	0.000005616	0.891821992
sample	0.1229	9.26E-13	0.000001852	0.089182199
sample	0.792	7.617E-12	0.000015234	0.00891822
sample	0.0729	4.26E-13	0.000000852	0.000891822
sample	0.0666	3.63E-13	0.000000726	8.91822E-05
sample	0.0804	5.01E-13	0.000001002	8.91822E-06
No DAT	0.0645	3.42E-13		
No DAT - reduced	0.074	4.37E-13		
sample	0.065	3.47E-13	0.000000694	8.918219923
sample	0.0676	3.73E-13	0.000000746	0.891821992
sample	0.0684	3.81E-13	0.000000762	0.089182199
sample	0.0725	4.22E-13	0.000000844	0.00891822
sample	0.1001	6.98E-13	0.000001396	0.000891822
sample	0.0668	3.65E-13	0.00000073	8.91822E-05
sample	0.0645	3.42E-13	0.000000684	8.91822E-06

Data Table 19: 6/10/2013, Average and standard deviation of 61013

New Tube	µmoles in	Average µmoles out	Standard Deviation
5,14 61013	8.918219923	0.000001112	5.91141E-07
6,15 61013	0.891821992	0.000003181	3.44361E-06
7,16 61013	0.089182199	0.000001307	7.70746E-07
8,17 61013	0.00891822	0.000008039	1.01753E-05
9,18 61013	0.000891822	0.000001124	3.84666E-07
10,19 61013	8.91822E-05	0.000000728	2.82843E-09
11,20 61013	8.91822E-06	0.000000843	2.2486E-07

Data Table 20: 6/10/2013, Self-titration with DAT description

Old Tube	New Tube	Description	GP (mg)	DAT (µg)
	1 61213	Just buffer	0	0
	2 61213	Just Ellman's and buffer	0	0
2 6113	3 61213	No DAT	0	0
2 61113	4 61213	No DAT - reduced	0	0
3 61113	5 61213	sample	0	2000
4 61113	6 61213	sample	0	200
5 61113	7 61213	sample	0	20
6 61113	8 61213	sample	0	2
7 61113	9 61213	sample	0	0.2
8 61113	10 61213	sample	0	0.02
9 61113	11 61213	sample	0	0.002

Data Table 21: 6/12/2013, GP titration with DAT description

Old Tube	New Tube	Description	GP (mg)	DAT (µg)
	1 61313	Just buffer	0	0
	2 61313	Just Ellman's and buffer	0	0
2 61213	3 61313	No DAT	0.2	0
2 61213	4 61313	No DAT - reduced	0.2	0
3 61213	5 61313	sample	0.2	200
4 61213	6 61313	sample	0.2	20
5 61213	7 61313	sample	0.2	2
6 61213	8 61313	sample	0.2	0.2
7 61213	9 61313	sample	0.2	0.02
8 61213	10 61313	sample	0.2	0.002
2 61213	11 61313	No DAT	0.2	0
2 61213	12 61313	No DAT - reduced	0.2	0
3 61213	13 61313	sample	0.2	200
4 61213	14 61313	sample	0.2	20
5 61213	15 61313	sample	0.2	2
6 61213	16 61313	sample	0.2	0.2
7 61213	17 61313	sample	0.2	0.02
8 61213	18 61313	sample	0.2	0.002

Data Table 22: 6/12/2013, GP titration with DAT absorbance readings

Description	Absorbance	Calc. moles per well	Total µmoles out	µmol put in
Just buffer	0			
Just Ellman's and buffer	0.0542	2.39E-13		
No DAT	0.0705	4.02E-13		
No DAT - reduced	0.0682	3.79E-13		
sample	0.0697	3.94E-13	0.000000788	0.891821992
sample	0.0657	3.54E-13	0.000000708	0.089182199
sample	0.0663	3.6E-13	0.00000072	0.00891822
sample	0.0874	5.71E-13	0.000001142	0.000891822
sample	0.0723	4.2E-13	0.00000084	8.91822E-05
sample	0.0642	3.39E-13	0.000000678	8.91822E-06
No DAT	0.0657	3.54E-13		
No DAT - reduced	0.0777	4.74E-13		
sample	0.0789	4.86E-13	0.000000972	0.891821992
sample	0.074	4.37E-13	0.000000874	0.089182199
sample	0.0829	5.26E-13	0.000001052	0.00891822
sample	0.0704	4.01E-13	0.000000802	0.000891822
sample	0.0655	3.52E-13	0.000000704	8.91822E-05
sample	0.0833	5.3E-13	0.00000106	8.91822E-06

Data Table 23: 6/13/2013, Average and standard deviation of 61313

New Tube	µmol in	Average µmol out	Standard Deviation
5,13 61313	0.891821992	0.00000088	1.30108E-07
6,14 61313	0.089182199	0.000000791	1.1738E-07
7,15 61313	0.00891822	0.000000886	2.34759E-07
8,16 61313	0.000891822	0.000000972	2.40416E-07
9,17 61313	8.91822E-05	0.000000772	9.61665E-08
10,18 61313	8.91822E-06	0.000000869	2.70115E-07

Data Table 24: 6/17/2013, GP titration with DAT description

Old Tube	New Tube	Description	GP (mg)	DAT (µg)
	1 61813	Just buffer	0	0
	2 61813	Just Ellman's and buffer	0	0
2 61713	3 61813	No DAT	0.2	0
2 61713	4 61813	No DAT - reduced	0.2	0
3 61713	5 61813	sample	0.2	200
4 61713	6 61813	sample	0.2	20
5 61713	7 61813	sample	0.2	2
6 61713	8 61813	sample	0.2	0.2
7 61713	9 61813	sample	0.2	0.02
2 61713	10 61813	No DAT	0.2	0
2 61713	11 61813	No DAT - reduced	0.2	0
3 61713	12 61813	sample	0.2	200
4 61713	13 61813	sample	0.2	20
5 61713	14 61813	sample	0.2	2
6 61713	15 61813	sample	0.2	0.2
7 61713	16 61813	sample	0.2	0.02

Data Table 25: 6/17/13, GP titration with DAT absorbance readings

Description	Absorbance	Calc. mol per well	Total µmol out	µmol put in
Just buffer	0			
Just Ellman's and buffer	0.0384	8.1E-14		
No DAT	0.0388	8.5E-14		
No DAT - reduced	0.0612	3.09E-13		
sample	0.0472	1.69E-13	0.000000338	0.891821992
sample	0.0466	1.63E-13	0.000000326	0.089182199
sample	0.0471	1.68E-13	0.000000336	0.00891822
sample	0.0706	4.03E-13	0.000000806	0.000891822
sample	0.0554	2.51E-13	0.000000502	8.91822E-05
No DAT	0.0471	1.68E-13		
No DAT - reduced	0.1137	8.34E-13		
sample	0.0475	1.72E-13	0.000000344	0.891821992
sample	0.0453	1.5E-13	0.0000003	0.089182199
sample	0.2225	1.922E-12	0.000003844	0.00891822
sample	0.0537	2.34E-13	0.000000468	0.000891822
sample	0.0563	2.6E-13	0.00000052	8.91822E-05

Data Table 26: 6/17/2013, Average and standard deviation of 61713

New Tube	µmol in	Averave µmol out	Standard Deviation
5,12 61813	0.891821992	0.000000341	4.24264E-09
6,13 61813	0.089182199	0.000000313	1.83848E-08
7,14 61813	0.00891822	0.00000209	2.48053E-06
8,15 61813	0.000891822	0.000000637	2.39002E-07
9,16 61813	8.91822E-05	0.000000511	1.27279E-08

Data Table 27: 7/10/2013, GP titration with DAT description

Old Tube	New Tube	Description	GP (mg)	DAT (µg)	Reducing agent (µL, type)
	7 71013	Just buffer	0	0	0
	8 71013	Just Ellman's and buffer	0	0	0
1 71013	9 71013	No DAT - reduced	0.2	0	10, TCEP
2 71013	10 71013	sample	0.2	200	10, TCEP
3 71013	11 71013	sample	0.2	20	10, TCEP
4 71013	12 71013	sample	0.2	2	10, TCEP
5 71013	13 71013	sample	0.2	0.2	10, TCEP
6 71013	14 71013	sample	0.2	0.02	10, TCEP
1 71013	15 71013	No DAT - reduced	0.2	0	10, DTT
2 71013	16 71013	sample	0.2	200	10, DTT
3 71013	17 71013	sample	0.2	20	10, DTT
4 71013	18 71013	sample	0.2	2	10, DTT
5 71013	19 71013	sample	0.2	0.2	10, DTT
6 71013	20 71013	sample	0.2	0.02	10, DTT
1 71013	21 71013	No DAT - reduced	0.2	0	10, B-mercaptoethanol
2 71013	22 71013	sample	0.2	200	10, B-mercaptoethanol
3 71013	23 71013	sample	0.2	20	10, B-mercaptoethanol
4 71013	24 71013	sample	0.2	2	10, B-mercaptoethanol
5 71013	25 71013	sample	0.2	0.2	10, B-mercaptoethanol
6 71013	26 71013	sample	0.2	0.02	10, B-mercaptoethanol
1 71013	27 71013	No DAT - reduced	0.2	0	10, PBS
2 71013	28 71013	sample	0.2	200	10, PBS
3 71013	29 71013	sample	0.2	20	10, PBS
4 71013	30 71013	sample	0.2	2	10, PBS
5 71013	31 71013	sample	0.2	0.2	10, PBS
6 71013	32 71013	sample	0.2	0.02	10, PBS

Data Table 28: 7/10/2013, GP titration with DAT absorbance readings

Description	Absorbance	Calc. mol per well	Total µmol out	µmol put in
Just buffer	0			
Just Ellman's and buffer	0.0331	2.8E-14		
No cmpnd - reduced	0.0358	5.5E-14		
sample	0.0429	1.26E-13	0.000000252	0.891821992
sample	0.0425	1.22E-13	0.000000244	0.089182199
sample	0.0401	9.8E-14	0.000000196	0.00891822
sample	0.0406	1.03E-13	0.000000206	0.000891822
sample	0.0444	1.41E-13	0.000000282	8.91822E-05
No cmpnd - reduced	0.0373	7E-14	0.00000014	0
sample	0.046	1.57E-13	0.000000314	0.891821992
sample	0.0413	1.1E-13	0.00000022	0.089182199
sample	0.0405	1.02E-13	0.000000204	0.00891822
sample	0.0426	1.23E-13	0.000000246	0.000891822
sample	0.0424	1.21E-13	0.000000242	8.91822E-05
No cmpnd - reduced	0.0406	1.03E-13	0.000000206	0
sample	0.039	8.7E-14	0.000000174	0.891821992
sample	0.0398	9.5E-14	0.00000019	0.089182199
sample	0.0405	1.02E-13	0.000000204	0.00891822
sample	0.0434	1.31E-13	0.000000262	0.000891822
sample	0.0441	1.38E-13	0.000000276	8.91822E-05
No cmpnd - reduced	0.0382	7.9E-14	0.000000158	0
sample	0.0388	8.5E-14	0.00000017	0.891821992
sample	0.0387	8.4E-14	0.000000168	0.089182199
sample	0.0397	9.4E-14	0.000000188	0.00891822
sample	0.0381	7.8E-14	0.000000156	0.000891822
sample	0.0416	1.13E-13	0.000000226	8.91822E-05